On the use of Lamb modes in the linear sampling method for elastic waveguides

L. Bourgeois†, F. Le Louër†, E. Lunéville†
† Laboratoire POEMS, 32, Boulevard Victor, 75739 Paris Cedex 15, France

Abstract

This paper is devoted to a modal formulation of the Linear Sampling Method in elastic 2D or 3D waveguide, that is we use the guided modes (called Lamb modes in 2D) as incident waves and the corresponding far fields in order to retrieve some obstacles. We provide the mathematical background to tackle the problem of identifiability and the justification of the Linear Sampling Method for such case. The elastic waveguide raises a specific issue: it concerns the projection of the scattered field on a transverse basis, which requires the introduction of new variables that mix displacement and stress components and satisfy the so-called Fraser's biorthogonality condition. Some numerical experiments in 2D show the feasibility of the reconstruction in the case of a finite number of incident waves formed by Lamb modes.

1 Introduction

Ultrasonic non-destructive testing (NDT) is one of the most promising techniques to inspect structures. Assuming that the behaviour of the material is governed by a linear elastic constitutive law, which is for example the case of metallic structures in many applications, the appropriate model to study ultrasonic NDT is elastodynamics. When frequency is fixed, elastodynamics in the time-harmonic regime may be used, which is the simple case we consider in this paper.
A number of structures which have to be tested in an industrial context have at least one bounded dimension, for example thick plates, cables or pipes. Such structures are called waveguides. Because of the physical presence of the boundary, the waveguide modes are divided into two categories: a finite number of propagative modes, and an infinite number of evanescent modes. This fact makes NDT more challenging than in free space, because only the propagative modes travel at long distance without loss of energy. The non-accessible parts of the waveguide may be inspected by using such propagative modes as incident waves, but identifiability is not guaranteed.
The problem of finding some defects (impenetrable/penetrable obstacles, cracks,...) from the measurements of the far field generated by propagative modes may be viewed as an inverse problem. Among all the methods that can be used to solve such inverse problem, we consider the Linear Sampling Method (LSM), which is now well known since its introduction in the celebrated paper by Colton and Kirsch [13] and the publication

of the additional arguments in [14, 2, 3]. One may also find a large amount of possible applications of the LSM in [10], as well as applications of the Kirsch factorization method, which is strongly connected to the LSM, in [21]. The LSM has many interesting features, in particular the fact that the way it is computed is independent of the defect we wan't to retrieve. This fact will be illustrated once again in the numerical section of the present paper, which addresses the identification of both hard obstacles and cracks.

The LSM has already been successfully used in the context of isotropic elasticity, and we refer to [1, 2, 4, 11, 18, 19, 23] for a non-comprehensive list of theoretical and numerical studies involving either far field (in free space) or near field (in half-space). But is seems to the authors that limited attention has up to now been paid to the specific geometry of waveguides. In the simpler case of acoustics, the first and third authors have exposed in [8] how LSM can be adapted to waveguides that are bounded in all directions but one, by using a modal formulation that is specifically designed for such geometry. Note that the acoustic case in 2D may be viewed as the specific case of SH propagation in an elastic thick plate with invariance in one direction. It was shown in particular that for sufficiently large frequency, propagative modes are enough to retrieve obstacles in practice. When a finite number of modes are taken into account, the data may be viewed as a scattering matrix. It should also be noted that some recent communications have considered inverse scattering problems in acoustic waveguide from other points of view than LSM, for example [12, 15, 16].

The main ingredient of the modal formulation in [8] is the expansion of the acoustic field with respect to the transverse modes in the bounded section of the waveguide. It is natural to ask whether our approach may be extended to the framework of elasticity, in view of NDT applications. We claim the answer is yes, but we acknowledge that such extension requires a significant amount of additional technicalities we will detail in the paper. The reason is that, to the authors' knowledge, it is not possible to develop the displacement field with respect to the transverse modes as it was done for the acoustic field. Such issue is not specific to inverse problems. The computation of the forward problem in the elastic waveguide raises the same difficulty: in the framework of the finite element method for example, the definition of transparent boundary conditions also needs some expansion with respect to the transverse modes. In order to overcome such issue, we use a biorthogonality relationship between two hybrid variables that mix displacement and stress components. This relationship was first introduced by Fraser in [17], then used in [24] in 2D to solve forward problems by using an impedance matrix which is solution to a Riccati equation, and recently used in [6] to solve forward problems with the help of a finite element formulation based on transparent boundary conditions. Our contribution is aimed at merging the ingredients of both [6] and [8] in order to derive a modal formulation of the Linear Sampling Method for isotropic elastic waveguides based on the far field measurements, and showing that it is successful with the help of numerical tests in 2D. To simplify the presentation, the theoretical justifications are done in the case of hard obstacles (vanishing displacement on the boundary), though such limitation is not essential in our method.

We point out that the theoretical results we present in this paper rely on some conjectures we admit, essentially the completeness of the transverses modes in terms of the hybrid

variables and well-posedness of the formulation of the direct problem, which are both open problems to the authors' knowledge.
Our paper is organized as follows. In section two we introduce the formalism we consider to describe the forward scattering problem in the elastic waveguide, in particular the biorthogonality relationship. The computation of the guided modes in 2D are given in appendix A, and some technicalities related to the Green function are postponed in appendix B, C and D. Section 3 is devoted to the Linear Sampling Method in the elastic waveguide in 2D or 3D: we begin with a classical near field formulation for which we give the theoretical foundations, then derive a modal formulation using the guided modes as incident waves. Numerical experiments in 2D are eventually presented in section 4.

2 The scattering problem in an elastic waveguide

We consider a waveguide $W = S \times \mathbb{R}$ in $\mathbb{R}^d$ with $d = 2$ or $d = 3$. In 2D we assume that $S = (-h, h)$ where h is a positive real number and in 3D we consider that S is a bounded connected domain in $\mathbb{R}^2$ with a smooth boundary. We note $x = (x_S, x_3)$ each point in W where $x_S \in S$ and $x_3 \in \mathbb{R}$. For an isotropic material which is characterized by the Lamé coefficients λ, μ with $\lambda + 2\mu > 0$, $\mu > 0$ and the density $\rho > 0$, the time-harmonic elastic waves are governed by the system in W

$$\operatorname{div} \sigma(\mathbf{u}) + \rho\omega^2 \mathbf{u} = 0. \tag{2.1}$$

Assuming that the boundary of W is traction free, we have on ∂W

$$\sigma(\mathbf{u})\boldsymbol{\nu} = 0. \tag{2.2}$$

Here

$$\sigma(\mathbf{u}) = \lambda \operatorname{div}(\mathbf{u})\mathrm{I} + 2\mu\varepsilon(\mathbf{u}) \quad \text{and} \quad \varepsilon(\mathbf{u}) = \frac{1}{2}\left(\nabla\mathbf{u} + {}^T\nabla\mathbf{u}\right)$$

denote the stress tensor and the strain tensor respectively, $\boldsymbol{\nu}$ denotes the outer unit normal vector to W.

2.1 An evolution problem

We now introduce the formalism of [6] in the 3D case, having in mind that in the 2D case each component having the subscript 2 disappears. We first define $\boldsymbol{\nu}_S = (\nu_1, \nu_2)$, $\mathbf{u} = (\mathbf{u}_S, \mathsf{u}_3)$, $\sigma(\mathbf{u})e_3 = (\mathbf{t}_S, -\mathsf{t}_3)$,

$$\sigma_S = \begin{pmatrix} \sigma_{11} & \sigma_{12} \\ \sigma_{21} & \sigma_{22} \end{pmatrix}, \quad \varepsilon_S = \begin{pmatrix} \varepsilon_{11} & \varepsilon_{12} \\ \varepsilon_{21} & \varepsilon_{22} \end{pmatrix},$$

as well as our mixed variables:

$$\mathbf{X} = \begin{pmatrix} \mathbf{t}_S \\ \mathsf{u}_3 \end{pmatrix} \quad \text{and} \quad \mathbf{Y} = \begin{pmatrix} \mathbf{u}_S \\ \mathsf{t}_3 \end{pmatrix}.$$

By a straightforward calculation, we show that (2.1) and (2.2) are equivalent to the evolution problem:

$$\frac{\partial}{\partial x_3}\begin{pmatrix}\mathbf{X}\\ \mathbf{Y}\end{pmatrix}=\begin{pmatrix}0 & F\\ G & 0\end{pmatrix}\begin{pmatrix}\mathbf{X}\\ \mathbf{Y}\end{pmatrix}, \tag{2.3}$$

where

$$F\mathbf{Y}=\begin{pmatrix}-\operatorname{div}\sigma_S(\mathbf{Y})-\rho\omega^2\mathbf{u}_S\\ -\alpha\operatorname{div}_S\mathbf{u}_S-\dfrac{\alpha}{\lambda}\mathrm{t}_3\end{pmatrix}\quad\text{and}\quad G\mathbf{X}=\begin{pmatrix}\dfrac{\mathbf{t}_S}{\mu}-\nabla_S\mathrm{u}_3\\ \operatorname{div}_S\mathbf{t}_S+\rho\omega^2\mathrm{u}_3\end{pmatrix},$$

and the boundary conditions on ∂W:

$$\begin{cases}\sigma_S(\mathbf{Y})\boldsymbol{\nu}_S=0,\\ \mathbf{t}_S.\boldsymbol{\nu}_S=0.\end{cases} \tag{2.4}$$

Here $\sigma_S(\mathbf{Y})=(\delta\operatorname{div}_S\mathbf{u}_S-\alpha\mathrm{t}_3)\mathrm{I}+2\mu\varepsilon_S(\mathbf{u}_S)$, $\delta=\dfrac{2\lambda\mu}{\lambda+2\mu}$, $\alpha=\dfrac{\lambda}{\lambda+2\mu}$, $\operatorname{div}_S\mathbf{u}_S=\partial_{x_1}u_1+\partial_{x_2}u_2$ and $\nabla_S\phi=\partial_{x_1}\phi\,e_1+\partial_{x_2}\phi\,e_2$.

2.2 The guided modes

We define the guided modes as the solutions to (2.1)-(2.2) of the form

$$\mathbf{u}(x)=\boldsymbol{u}(x_S)e^{i\beta x_3}. \tag{2.5}$$

By using the mixed variables $\mathbf{X}$ and $\mathbf{Y}$, with

$$\begin{pmatrix}\mathbf{X}\\ \mathbf{Y}\end{pmatrix}=\begin{pmatrix}\boldsymbol{\mathcal{X}}(x_S)\\ \boldsymbol{\mathcal{Y}}(x_S)\end{pmatrix}e^{i\beta x_3},$$

from (2.3)-(2.4)-(2.5) we immediately establish that such problem amounts to the eigenvalue problem:

$$i\beta\begin{pmatrix}\boldsymbol{\mathcal{X}}\\ \boldsymbol{\mathcal{Y}}\end{pmatrix}=\begin{pmatrix}0 & F\\ G & 0\end{pmatrix}\begin{pmatrix}\boldsymbol{\mathcal{X}}\\ \boldsymbol{\mathcal{Y}}\end{pmatrix} \tag{2.6}$$

with boundary condition:

$$\begin{cases}\sigma_S(\boldsymbol{\mathcal{Y}})\boldsymbol{\nu}_S=0,\\ \mathcal{X}_1\nu_1+\mathcal{X}_2\nu_2=0.\end{cases} \tag{2.7}$$

The eigenvalue problem (2.6)-(2.7) clearly depends on the spectrum of operator A defined by

$$A=\begin{pmatrix}0 & F\\ G & 0\end{pmatrix},$$

which depends on those of F and G.
More precisely, the operators F and G may be considered as unbounded operators in $\mathbf{L}^2(S)=\big(L^2(S)\big)^3$. We set $V_X=(L^2(S))^2\times H^1(S)$ and $V_Y=(H^1(S))^2\times L^2(S)$ and define the domain $D(F)$ of F as

$$D(F)=\big\{\boldsymbol{\mathcal{Y}}=(\boldsymbol{u}_S,t_3)\in V_Y,\quad \operatorname{div}_S\sigma_S(\boldsymbol{\mathcal{Y}})\in(L^2(S))^2\text{ and }\sigma_S(\boldsymbol{\mathcal{Y}}_S)\boldsymbol{\nu}_S=0\text{ on }\partial W\big\}$$

and the domain $D(G)$ of G as

$$D(G) = \left\{ \boldsymbol{\mathcal{X}} = (\boldsymbol{t}_S, u_3) \in V_X, \quad \mathrm{div}_S\, \boldsymbol{t}_S \in L^2(S) \text{ and } \boldsymbol{t}_S \cdot \boldsymbol{\nu}_S = 0 \text{ on } \partial W \right\}.$$

Lastly we define the bilinear form for $\boldsymbol{\mathcal{X}}, \boldsymbol{\mathcal{Y}} \in \mathbf{L}^2(S)$,

$$(\boldsymbol{\mathcal{X}}|\boldsymbol{\mathcal{Y}})_S = \int_S (\mathcal{X}_1\mathcal{Y}_1 + \mathcal{X}_2\mathcal{Y}_2 + \mathcal{X}_3\mathcal{Y}_3)\, dS = \int_S (\boldsymbol{u}_S \cdot \boldsymbol{t}_S + t_3 u_3)\, dS. \tag{2.8}$$

The form $(.|.)_S$ can clearly be extended to the case when $\boldsymbol{\mathcal{X}} \in (H^{-1/2}(S))^2 \times H^{1/2}(S)$ and $\boldsymbol{\mathcal{Y}} \in (H^{1/2}(S))^2 \times H^{-1/2}(S)$, which will be done in the sequel without change in the notations. Here $H^{-1/2}(S)$ is defined as the dual space of $H^{1/2}(S)$.

Remark 2.1 *For complex-valued functions, the form $(.|.)_S$ does not define an inner product of $\mathbf{L}^2(S)$. But on the one hand the following properties of operators F and G are true with $(.|.)_S$ because F and G have real coefficients, and on the other hand $(.|.)_S$ is preferable because of the biorthogonality relation hereafter.*

The useful properties of F and G, which are proved in [6], are summarized in the following proposition.

Proposition 2.2 *The operators F and G have the following properties:*

1. *The domains $D(F)$ and $D(G)$ are dense in $\mathbf{L}^2(S)$.*
2. *F and G are symmetric with respect to the bilinear form (2.8).*
3. *Except for a countable set of frequencies ω, F and G are self-adjoint.*
4. *Except for a countable set of frequencies ω, FG and GF have compact resolvent.*

By applying operator A to the system (2.6), it follows that

$$-\beta^2 \begin{pmatrix} \boldsymbol{\mathcal{X}} \\ \boldsymbol{\mathcal{Y}} \end{pmatrix} = \begin{pmatrix} FG & 0 \\ 0 & GF \end{pmatrix} \begin{pmatrix} \boldsymbol{\mathcal{X}} \\ \boldsymbol{\mathcal{Y}} \end{pmatrix}. \tag{2.9}$$

The operator A has the following properties:

Corollary 2.3 *Except for a countable set of frequencies ω, the operator A^2 has compact resolvent, hence the spectrum of A consists of a discrete set of eigenvalues with finite multiplicity.*

Throughout the paper we will assume the following.

Assumption 2.4 *The frequency ω is chosen such that points 3 and 4 of proposition 2.2 are true and that there is no eigensolution $(\beta, \boldsymbol{\mathcal{X}}, \boldsymbol{\mathcal{Y}})$ of system (2.6)-(2.7) satisfying $(\boldsymbol{\mathcal{X}}|\boldsymbol{\mathcal{Y}})_S = 0$.*

Under the above assumption, the eigenmodes of system (2.6)-(2.7) can be organized in two families:

1. the rightgoing modes $(\beta_n, \boldsymbol{\mathcal{X}}_n, \boldsymbol{\mathcal{Y}}_n)_{n>0}$, which correspond to $\Im(\beta_n) > 0$ (for non-propagative modes) or $\dfrac{\partial \omega}{\partial \beta_n} > 0$ (for propagative modes),
2. the leftgoing modes $(\beta_{-n}, \boldsymbol{\mathcal{X}}_{-n}, \boldsymbol{\mathcal{Y}}_{-n})_{n>0} = (-\beta_n, -\boldsymbol{\mathcal{X}}_n, \boldsymbol{\mathcal{Y}}_n)_{n>0}$.

The non-propagative modes can themselves be split into evanescent modes (β_n is purely imaginary) and inhomogeneous modes (β_n is not purely imaginary).

Remark 2.5 *It should be noted that $(-\beta_n^2, \boldsymbol{\mathcal{X}}_n, \boldsymbol{\mathcal{Y}}_n)$ are the eigensolutions of system (2.9), but since FG (resp. GF) is not self-adjoint, the family $\boldsymbol{\mathcal{X}}_n$ (resp. $\boldsymbol{\mathcal{Y}}_n$) is not orthogonal.*

But using self-adjointness of F and G (see [6]), we obtain the following biorthogonality relationship

$$(\boldsymbol{\mathcal{X}}_n | \boldsymbol{\mathcal{Y}}_m)_S = (\boldsymbol{u}_S^n, \boldsymbol{t}_S^m)_S + (u_3^n, t_3^m)_S = \delta_{nm} J_n,$$

where $J_n \neq 0$ is the Fraser's constant. In the 2D case, the eigenmodes $(\beta_n, \boldsymbol{\mathcal{X}}_n, \boldsymbol{\mathcal{Y}}_n)$ for $n > 0$ are the so-called lamb modes and can be computed analytically (see [5]). Since we need them in the numerical section, they are given in appendix A.

From now on, we use one normalization for the modes $\boldsymbol{\mathcal{X}}_n$ and $\boldsymbol{\mathcal{Y}}_n$ in such a way that

$$(\boldsymbol{\mathcal{X}}_n | \boldsymbol{\mathcal{Y}}_m)_S = \delta_{nm},$$

which amounts to assume that $J_n = 1$ for $n > 0$.
We now introduce an important completeness assumption.

Assumption 2.6 *For every $\boldsymbol{\mathcal{X}} = (\boldsymbol{t}_S, u_3) \in (H^{-1/2}(S))^2 \times H^{1/2}(S)$ we have*

$$\boldsymbol{\mathcal{X}} = \sum_{n \in \mathbb{N}^*} (\boldsymbol{\mathcal{X}} | \boldsymbol{\mathcal{Y}}_n)_S \boldsymbol{\mathcal{X}}_n, \tag{2.10}$$

for every $\boldsymbol{\mathcal{Y}} = (\boldsymbol{u}_S, t_3) \in (H^{1/2}(S))^2 \times H^{-1/2}(S)$ we have

$$\boldsymbol{\mathcal{Y}} = \sum_{n \in \mathbb{N}^*} (\boldsymbol{\mathcal{X}}_n | \boldsymbol{\mathcal{Y}})_S \boldsymbol{\mathcal{Y}}_n, \tag{2.11}$$

and there exists $c, C > 0$ such that

$$c\left(||\boldsymbol{t}_S||^2_{(H^{-1/2}(S))^2} + ||u_3||^2_{H^{1/2}(S)}\right) \leq \sum_{n \in \mathbb{N}^*} |(\boldsymbol{\mathcal{X}} | \boldsymbol{\mathcal{Y}}_n)_S|^2 \leq C\left(||\boldsymbol{t}_S||^2_{(H^{-1/2}(S))^2} + ||u_3||^2_{H^{1/2}(S)}\right)$$

$$c\left(||\boldsymbol{u}_S||^2_{(H^{1/2}(S))^2} + ||t_3||^2_{H^{-1/2}(S)}\right) \leq \sum_{n \in \mathbb{N}^*} |(\boldsymbol{\mathcal{X}}_n | \boldsymbol{\mathcal{Y}})_S|^2 \leq C\left(||\boldsymbol{u}_S||^2_{(H^{1/2}(S))^2} + ||t_3||^2_{H^{-1/2}(S)}\right).$$

Decompositions (2.10) and (2.11) are also true for $\boldsymbol{\mathcal{X}} = (\boldsymbol{t}_S, u_3) \in \mathbf{L}^2(S)$ and $\boldsymbol{\mathcal{Y}} = (\boldsymbol{u}_S, t_3) \in \mathbf{L}^2(S)$.

Remark 2.7 *To the authors' knowledge, a rigorous proof of the above completeness statement is unknown in the general case.*

With the help of previous assumption, we have the following lemma.

Lemma 2.8 *The solutions to the problem (2.3)-(2.4) are given by*

$$\begin{pmatrix} \mathbf{X} \\ \mathbf{Y} \end{pmatrix} = \sum_{n>0} a_n^+ \begin{pmatrix} \mathbf{X}_n^+ \\ \mathbf{Y}_n^+ \end{pmatrix} + a_n^- \begin{pmatrix} \mathbf{X}_n^- \\ \mathbf{Y}_n^- \end{pmatrix} \tag{2.12}$$

with

$$\begin{pmatrix} \mathbf{X}_n^\pm(x) \\ \mathbf{Y}_n^\pm(x) \end{pmatrix} = \begin{pmatrix} \pm\boldsymbol{\mathcal{X}}_n(x_S) \\ \boldsymbol{\mathcal{Y}}_n(x_S) \end{pmatrix} e^{\pm i\beta_n x_3}. \tag{2.13}$$

Proof. By using assumption 2.6 we have

$$\begin{cases} \mathbf{X}(x_S, x_3) = \sum_{n>0} c_n(x_3)\boldsymbol{\mathcal{X}}_n(x_S) \\ \mathbf{Y}(x_S, x_3) = \sum_{n>0} d_n(x_3)\boldsymbol{\mathcal{Y}}_n(x_S). \end{cases}$$

By using (2.3) it follows that

$$\begin{cases} \sum_{n>0} c_n'(x_3)\boldsymbol{\mathcal{X}}_n(x_S) = \sum_{n>0} d_n(x_3) F\boldsymbol{\mathcal{Y}}_n \\ \sum_{n>0} d_n'(x_3)\boldsymbol{\mathcal{Y}}_n(x_S) = \sum_{n>0} c_n(x_3) G\boldsymbol{\mathcal{X}}_n. \end{cases}$$

From (2.6), it follows that $F\boldsymbol{\mathcal{Y}}_n = (i\beta_n)\boldsymbol{\mathcal{X}}_n$ and $G\boldsymbol{\mathcal{X}}_n = (i\beta_n)\boldsymbol{\mathcal{Y}}_n$, and by using now the biorthogonality relationship we obtain that for all n

$$\begin{cases} c_n'(x_3) = i\beta_n d_n(x_3) \\ d_n'(x_3) = i\beta_n c_n(x_3), \end{cases}$$

that is

$$c_n(x_3) = a_n^+ e^{i\beta_n x_3} - a_n^- e^{-i\beta_n x_3} \quad d_n(x_3) = a_n^+ e^{i\beta_n x_3} + a_n^- e^{-i\beta_n x_3},$$

which is the expansion (2.12). Conversely, the series given by (2.12) is a solution to (2.3)-(2.4). ■

We also denote

$$\mathbf{U}_n^\pm(x) = \begin{pmatrix} \boldsymbol{u}_S^n(x_S) \\ \pm u_3^n(x_S) \end{pmatrix} e^{\pm i\beta_n x_3},$$

which are the guided modes in term of displacement.

Remark 2.9 *It should be noted that $(\boldsymbol{u}_S^n, u_3^n)_{n>0}$ and $(\boldsymbol{u}_S^n, -u_3^n)_{n>0}$ do not separately form an orthogonal complete basis of $\mathbf{L}^2(S)$ or $\mathbf{H}^{\frac{1}{2}}(\partial\mathcal{D}) := (H^{\frac{1}{2}}(\partial\mathcal{D}))^3$.*

2.3 The scattering problem

We define $S_R = S \times \{R\}$ for $R \in \mathbb{R}$, W_R as the region of W between S_{-R} and S_R, Γ_R as the region of ∂W between S_{-R} and S_R. Let $\mathcal{D}$ be a bounded domain in W with Lipschitz continuous boundary $\partial\mathcal{D}$, referred to as the obstacle (see figure 1). This obstacle is assumed to lie between S_{-R_0} and S_{R_0} with $R_0 > 0$. For $\boldsymbol{f} \in \mathbf{H}^{\frac{1}{2}}(\partial\mathcal{D})$ we consider the scattering problem in the presence of a hard obstacle for $R > R_0$: find $\mathbf{u} \in \mathbf{H}^1(W_R) := (H^1(W_R))^3$ such that

$$\left\{\begin{array}{rcll} \operatorname{div}\sigma(\mathbf{u}) + \rho\omega^2\mathbf{u} & = & 0 & \text{in } W_R \\ \sigma(\mathbf{u})\boldsymbol{\nu} & = & 0 & \text{on } \Gamma_R \\ \mathbf{u} & = & \boldsymbol{f} & \text{on } \partial\mathcal{D} \\ T^{\pm}\mathbf{Y} & = & \pm\mathbf{X} & \text{on } S_{\pm R} \end{array}\right. \tag{2.14}$$

where

$$T^{\pm}\mathbf{Y} = \sum_{n>0} (\boldsymbol{\mathcal{X}}_n|\mathbf{Y})_{S_{\pm R}} \boldsymbol{\mathcal{X}}_n,$$

that is in a more explicit way

$$T^{\pm}\begin{pmatrix} \mathbf{u}_S \\ \mathsf{t}_3 \end{pmatrix} = \begin{pmatrix} \sum_{n>0}(\boldsymbol{t}_S^n, \mathbf{u}_S)_{S_{\pm R}} \boldsymbol{t}_S^n & \sum_{n>0}(u_3^n, \mathsf{t}_3)_{S_{\pm R}} \boldsymbol{t}_S^n \\ \sum_{n>0}(\boldsymbol{t}_S^n, \mathbf{u}_S)_{S_{\pm R}} u_3^n & \sum_{n>0}(u_3^n, \mathsf{t}_3)_{S_{\pm R}} u_3^n \end{pmatrix}.$$

The last equation in the system (2.14) is the radiation condition, which selects an outgoing solution. Such radiation condition is obtained by prescribing that for $x_3 > R$, the solution is of the form (2.12) with $a_n^- = 0$, and for $x_3 < -R$, the solution is of the form (2.12) with $a_n^+ = 0$. Assumption 2.6 implies that operator T is continuous. In the remainder of the paper we suppose that

Assumption 2.10 *The frequency ω is chosen such that problem (2.14) is well-posed.*

A weak formulation of problem (2.14) is given in [6], which will be used in the numerical section of the present paper in order to obtain artificial data. To the authors' knowledge, well-posedness of problem (2.14) is still an open problem, even if we make the completeness assumption 2.6.

2.4 The Green tensor

The Linear Sampling Method is strongly linked to the singularity of the Green tensor in the waveguide. That is why we have to explicit such Green tensor, in particular in the formalism of mixed variables.

We first need to define some extension and restriction operators. We denote $\mathcal{E}|_{XY} : \mathbf{H}^1(W_R) \to (L^2(W_R))^2 \times H^1(W_R) \times (H^1(W_R))^2 \times L^2(W_R)$ the extension operator defined for a displacement field $\mathbf{u}$ by

$$\mathcal{E}|_{XY}\mathbf{u} = \begin{pmatrix} \mathbf{t}_S \\ \mathsf{u}_3 \\ \mathbf{u}_S \\ \mathsf{t}_3 \end{pmatrix} = \begin{pmatrix} \mathbf{X} \\ \mathbf{Y} \end{pmatrix}.$$

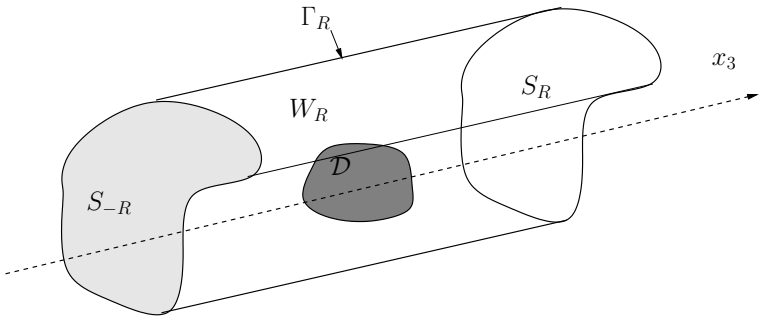

Figure 1: Notations for the direct problem

We denote by $\mathcal{R}|_u : (L^2(W_R))^2 \times H^1(W_R) \times (H^1(W_R))^2 \times L^2(W_R) \to \mathbf{H}^1(W_R)$ the restriction operator defined for a couple $(\mathbf{X}, \mathbf{Y})$ by

$$\mathcal{R}|_u \begin{pmatrix} \mathbf{X} \\ \mathbf{Y} \end{pmatrix} = \mathcal{R}|_u \begin{pmatrix} \mathbf{t}_S \\ \mathsf{u}_3 \\ \mathbf{u}_S \\ \mathsf{t}_3 \end{pmatrix} = \begin{pmatrix} \mathbf{u}_S \\ \mathsf{u}_3 \end{pmatrix} = \mathbf{u}.$$

We define in the same way $\mathcal{R}|_\sigma$, $\mathcal{R}|_X$ and $\mathcal{R}|_Y$ the restriction operators of $(\mathbf{X}, \mathbf{Y})$ to $\sigma(\boldsymbol{u})e_3$, $\mathbf{X}$ and $\mathbf{Y}$ respectively. All these restriction and extension operators are continuous. We can extend the operators $\mathcal{E}$ and $\mathcal{R}$ from vector spaces to tensor spaces, by specifying with a ^{x} or a ^{y} if the operation concerns the lines or the columns of the tensor.
The classical outgoing Green tensor of the elastic waveguide W, denoted $G_u^\sigma(\cdot, y)$ for some given point $y = (y_S, y_3) \in W$, is the solution to the following problem, for $R > R_0$:

$$\left\{ \begin{array}{rcll} \operatorname{div} \sigma(G_u^\sigma(\cdot, y)) + \rho\omega^2 G_u^\sigma(\cdot, y) & = & \delta(. - y)\mathrm{I}_3 & \text{in } W \\ \sigma(G_u^\sigma(\cdot, y))\boldsymbol{\nu} & = & 0 & \text{on } \partial W \\ T^\pm \mathcal{R}^x|_Y \mathcal{E}|^x_{XY} G_u^\sigma(., y) & = & \pm \mathcal{R}^x|_X \mathcal{E}^x|_{XY} G_u^\sigma(\cdot, y) & \text{on } S_{\pm R}. \end{array} \right. \tag{2.15}$$

In order to formulate the linear sampling method in the framework of mixed variables $(\mathbf{X}, \mathbf{Y})$ (see next section), we also need to define the extended outgoing Green tensor of the elastic waveguide W, denoted $G(\cdot, y)$, which is the solution to the following problem, for $R > R_0$:

$$\left\{ \begin{array}{c} \dfrac{\partial}{\partial x_3} G(\cdot, y) = \begin{pmatrix} 0 & F \\ G & 0 \end{pmatrix} G(\cdot, y) + \delta(\cdot - y) \begin{pmatrix} \mathrm{I}_3 & 0_3 \\ 0_3 & \mathrm{I}_3 \end{pmatrix} \quad \text{in } W \\ \sigma_S(G(\cdot, y))\boldsymbol{\nu}_S = 0 \quad \mathbf{t}_S(G(\cdot, y)).\boldsymbol{\nu}_S = 0 \quad \text{on } \partial W \\ T^\pm \mathcal{R}^x|_Y G(\cdot, y) = \pm \mathcal{R}^x|_X G(\cdot, y) \quad \text{on } S_{\pm R}. \end{array} \right. \tag{2.16}$$

It is easy to prove by transforming the system (2.15) into an evolution system that G_u^σ may be obtained from G by applying the operator $\mathcal{R}|_u$ with respect to the variable x and by applying the operator $\mathcal{R}|_\sigma$ with respect to the variable y, namely

$$\mathcal{R}^x|_u \mathcal{R}^y|_\sigma G(x, y) = G_u^\sigma(x, y). \tag{2.17}$$

Now we exhibit an explicit form of tensor G in the following proposition, the proof of which is given in appendix B.

Proposition 2.11 *The tensor G is given by*

$$G = \begin{pmatrix} G_X^X & G_X^Y \\ G_Y^X & G_Y^Y \end{pmatrix},$$

with

$$G_X^X(x,y) = s(x_3-y_3)\sum_{n>0}\begin{pmatrix} t_1^n(x_S)u_1^n(y_S) & t_1^n(x_S)u_2^n(y_S) & t_1^n(x_S)t_3^n(y_S) \\ t_2^n(x_S)u_1^n(y_S) & t_2^n(x_S)u_2^n(y_S) & t_2^n(x_S)t_3^n(y_S) \\ u_3^n(x_S)u_1^n(y_S) & u_3^n(x_S)u_2^n(y_S) & u_3^n(x_S)t_3^n(y_S) \end{pmatrix}\frac{e^{i\beta_n|x_3-y_3|}}{2}$$

$$G_X^Y(x,y) = \sum_{n>0}\begin{pmatrix} t_1^n(x_S)t_1^n(y_S) & t_1^n(x_S)t_2^n(y_S) & t_1^n(x_S)u_3^n(y_S) \\ t_2^n(x_S)t_1^n(y_S) & t_2^n(x_S)t_2^n(y_S) & t_2^n(x_S)u_3^n(y_S) \\ u_3^n(x_S)t_1^n(y_S) & u_3^n(x_S)t_2^n(y_S) & u_3^n(x_S)u_3^n(y_S) \end{pmatrix}\frac{e^{i\beta_n|x_3-y_3|}}{2}$$

$$G_Y^X(x,y) = \sum_{n>0}\begin{pmatrix} u_1^n(x_S)u_1^n(y_S) & u_1^n(x_S)u_2^n(y_S) & u_1^n(x_S)t_3^n(y_S) \\ u_2^n(x_S)u_1^n(y_S) & u_2^n(x_S)u_2^n(y_S) & u_2^n(x_S)t_3^n(y_S) \\ t_3^n(x_S)u_1^n(y_S) & t_3^n(x_S)u_2^n(y_S) & t_3^n(x_S)t_3^n(y_S) \end{pmatrix}\frac{e^{i\beta_n|x_3-y_3|}}{2}$$

$$G_Y^Y(x,y) = s(x_3-y_3)\sum_{n>0}\begin{pmatrix} u_1^n(x_S)t_1^n(y_S) & u_1^n(x_S)t_2^n(y_S) & u_1^n(x_S)u_3^n(y_S) \\ u_2^n(x_S)t_1^n(y_S) & u_2^n(x_S)t_2^n(y_S) & u_2^n(x_S)u_3^n(y_S) \\ t_3^n(x_S)t_1^n(y_S) & t_3^n(x_S)t_2^n(y_S) & t_3^n(x_S)u_3^n(y_S) \end{pmatrix}\frac{e^{i\beta_n|x_3-y_3|}}{2},$$

where s is the sign function.

It follows from (2.17) that

$$G_u^\sigma(x,y) = \sum_{n>0}\begin{pmatrix} u_1^n(x_S)u_1^n(y_S) & u_1^n(x_S)u_2^n(y_S) & -s(x_3-y_3)u_1^n(x_S)u_3^n(y_S) \\ u_2^n(x_S)u_1^n(y_S) & u_2^n(x_S)u_2^n(y_S) & -s(x_3-y_3)u_2^n(x_S)u_3^n(y_S) \\ s(x_3-y_3)u_3^n(x_S)u_1^n(y_S) & s(x_3-y_3)u_3^n(x_S)u_2^n(y_S) & -u_3^n(x_S)u_3^n(y_S) \end{pmatrix}\frac{e^{i\beta_n|x_3-y_3|}}{2}.$$

We clearly have the following symmetry relationship

$$G_u^\sigma(x,y) = {}^T G_u^\sigma(y,x),$$

and by denoting $G_u^Y(x,y) = \mathcal{R}^x|_u\mathcal{R}^y|_Y G(x,y)$ and $G_X^\sigma(x,y) = \mathcal{R}^x|_X\mathcal{R}^y|_\sigma G(x,y)$,

$$G_u^Y(x,y) = -{}^T G_X^\sigma(y,x).$$

This last unusual symmetry relationship will play a crucial role in the justification of the Linear Sampling Method.

Now we recall some useful properties of the Green tensor G. First of all, we analyze the singularity of $G_u^\sigma(.,y)$ by comparing it with the singularity of the Green tensor of elasticity in free space, denoted $E(.,y)$. The tensor $E(\cdot,y)$ is for fixed $y \in \mathbb{R}^d$ $(d=2,3)$ the solution of the system

$$\operatorname{div}\sigma(E(\cdot,y)) + \rho\omega^2 E(\cdot,y) = \delta(\cdot-y)\mathrm{I}_3$$

satisfying a classical radiation condition for elasticity. The following lemma specifies the singularity of the Green tensor $G_u^\sigma(.,y)$.

Lemma 2.12 *(singularity of the Green tensor) The singularity of G_u^σ in the vicinity $x = y$ is like $log(|x-y|)$ in 2D and $1/|x-y|$ in 3D.*

PROOF. For $y \in W$ the function $G_u^\sigma(\cdot, y) - E(\cdot, y)$ satisfies the homogeneous time-harmonic elastic equations in W. As a consequence $G_u^\sigma(\cdot, y) - E(\cdot, y)$ is a smooth function in W and $G_u^\sigma(x, y)$ behaves as $E(x, y)$ when $|x-y| \to 0$. Defining $g_k(x, y) = -\frac{i}{4} H_0^1(\kappa|x-y|)$ in $2D$ and $g_\kappa(x, y) = -\frac{e^{i\kappa|x-y|}}{4\pi|x-y|}$ in $3D$, it is proved in [20] that the Green tensor $E(x, y)$ is given by

$$\mu E(x, y) = g_{k_s}(x, y)\mathrm{I}_3 + \frac{1}{k_s^2}\mathrm{Hess}(g_{k_s} - g_{k_p}),$$

where Hess denotes the Hessian,

$$k_S = \omega\sqrt{\frac{\rho}{\mu}}, \quad k_P = \omega\sqrt{\frac{\rho}{\lambda + 2\mu}}.$$

That the singularity of E is like $\log(|x-y|)$ in 2D (see [2]) and $1/|x-y|$ in 3D (see [20]) completes the proof. ■

Next, we need an integral representation result for the solution of the scattering problem (2.14) with some $\boldsymbol{f} \in \mathbf{H}^{1/2}(\partial\mathcal{D})$. In this view we recall the following well-known Green formula:

Lemma 2.13 *(integration by parts) Let Ω be a Lipschitz bounded domain of $\mathbb{R}^d$ and let $\mathbf{u}$ and $\mathbf{v}$ in $\mathbf{H}^1(\Omega)$ with $\operatorname{div}\sigma(\mathbf{u})$ and $\operatorname{div}\sigma(\mathbf{v})$ in $\mathbf{L}^2(\Omega)$, then we have*

$$\int_\Omega (\operatorname{div}\sigma(\mathbf{u}).\mathbf{v} - \operatorname{div}\sigma(\mathbf{v}).\mathbf{u})\, dx = \int_{\partial\Omega} (\sigma(\mathbf{u})\boldsymbol{\nu}\cdot\mathbf{v} - \sigma(\mathbf{v})\boldsymbol{\nu}\cdot\mathbf{u})\, ds,$$

where $\boldsymbol{\nu}$ is the outer unit normal vector to Ω.

In the above integration by parts formula, the integral in the right-hand side has to be understood in the sense of duality pairing between $\mathbf{H}^{-1/2}(\partial\Omega)$ and $\mathbf{H}^{1/2}(\partial\Omega)$, the first space being the dual of the second one. In the following we will note with an integral such kind of duality pairing for sake of simplicity, except in the case we have to better emphasize this duality pairing for clarity.
The following integral representation formula is proved in appendix C.

Lemma 2.14 *(integral representation) Let $\mathbf{u}$ be the solution of the scattering problem (2.14) with $f \in \mathbf{H}^{\frac{1}{2}}(\partial\mathcal{D})$. For all $x \in W \setminus \overline{\mathcal{D}}$ we have*

$$\mathbf{u}(x) = \int_{\partial\mathcal{D}} (\gamma_\nu^y(G_u^\sigma(x, y))\mathbf{u}(y) - G_u^\sigma(x, y)\gamma_\nu\mathbf{u}(y))\, ds(y),$$

where $\gamma_\nu(\mathbf{u}) = \sigma(\mathbf{u})\boldsymbol{\nu}$, with $\boldsymbol{\nu}$ the outer unit normal vector to $W \setminus \overline{\mathcal{D}}$ and $\gamma_\nu^y(G_u^\sigma(x, y))$ is the tensor the line number i of which is formed by $\gamma_\nu^y(G_{u,i}^\sigma(x, y))$, where $G_{u,i}^\sigma(x, y)$ is the line number i of tensor $G_u^\sigma(x, y)$.

We conclude this review of properties of tensor G with a reciprocity property which is proved in appendix D.

Lemma 2.15 *(reciprocity) We denote by $U^s_Y(\cdot, y)$ the solution of the scattering problem (2.14) with $f = -G^Y_u(\cdot, y)|_{\partial\mathcal{D}}$ for $y \in W\backslash\overline{\mathcal{D}}$. We also denote $X^s_\sigma(., y) = \mathcal{R}^x|_X\mathcal{E}^x|_{XY}U^s_\sigma(., y)$, where $U^s_\sigma(\cdot, y)$ is the solution of the scattering problem (2.14) with $f = -G^\sigma_u(\cdot, y)|_{\partial\mathcal{D}}$ for $y \in W \setminus \overline{\mathcal{D}}$. For all $x, y \in W \setminus \overline{\mathcal{D}}$ we have*

$$U^s_Y(x, y) = -{}^T X^s_\sigma(y, x).$$

3 The linear sampling method

3.1 The near field formulation

Let $R > R_0$. We consider the following two cases:

$$\begin{array}{ll} (i) & \hat{S} = S_R \\ (ii) & \hat{S} = S_{-R} \cup S_R. \end{array}$$

The case (i) will be called the full-aperture situation while case (ii) will be called the back-scattering situation.
We consider the incident waves $U^i(\cdot, y) = \mathcal{R}^x|_u\mathcal{R}^y|_Y G(\cdot, y) = G^Y_u(., y)$ for $y \in \hat{S}$, and we denote by $U^s_Y(., y)$ the corresponding scattered field due to the obstacle $\mathcal{D}$, with $X^s_Y(., y) := \mathcal{R}^x|_X\mathcal{E}^x|_{XY}U^s_Y(., y)$. In other words, $U^s_Y(., y)$ is the solution of problem (2.14) with $f = -U^i(\cdot, y)$. The corresponding total field is $U_Y(., y) = U^i(\cdot, y) + U^s_Y(., y)$, and the obstacle is hence characterized by vanishing displacement $U_Y(., y) = 0$ on $\partial\mathcal{D}$. In the following such obstacle will be referred to as a hard obstacle. The objective is to determine $\mathcal{D}$ from the measurements of $X^s_Y(\cdot, y)$ on $\hat{S}$ for all $y \in \hat{S}$.
We begin with a uniqueness result, that is unique determination of the obstacle from our measurements.

Theorem 3.1 *Let us denote by $\mathcal{D}_1$ and $\mathcal{D}_2$ two hard obstacles whose boundaries are either $C^{1,1}$ or polyhedral ($d = 3$)/polygonal ($d = 2$). If we assume that for all incident waves $U^i(., y) = G^Y_u(., y)$ with $y \in \hat{S}$, the corresponding scattered fields $X^s_{Y,1}(\cdot, y)$ and $X^s_{Y,2}(\cdot, y)$ coincide on $\hat{S}$, then $\mathcal{D}_1 = \mathcal{D}_2$.*

Proof. The proof is strongly inspired by the one of [25] and is based on our reciprocity lemma 2.15. It is enough to consider the back-scattering situation, that is $\hat{S} = S_R$. Assume that $X^s_{Y,1}(\cdot, y) = X^s_{Y,2}(\cdot, y)$ on S_R, and consider the solution $\tilde{X}^s(., y) = X^s_{Y,1}(\cdot, y) - X^s_{Y,2}(\cdot, y)$ in the domain $x_3 > R$ of the waveguide W. Proceeding as in the proof of lemma 2.8, the outgoing solution $(\tilde{X}^s, \tilde{Y}^s)(., y)$ can be written: for $x_3 > R$

$$\begin{pmatrix} \tilde{X}^s \\ \tilde{Y}^s \end{pmatrix} = \sum_{n>0} a^+_n \begin{pmatrix} \boldsymbol{\mathcal{X}}_n(x_S) \\ \boldsymbol{\mathcal{Y}}_n(x_S) \end{pmatrix} e^{i\beta_n x_3}.$$

Multiplying the first equation by $\boldsymbol{\mathcal{Y}}_n$ and integrating over S_R, it follows that for all $n > 0$,

$$(\tilde{X}^s|\boldsymbol{\mathcal{Y}}_n)_{S_R} = a_n^+ e^{i\beta_n R}.$$

Since $\tilde{X}^s(.,y) = 0$ on S_R it follows that $a_n^+ = 0$ and $\tilde{X}^s(.,y)$ vanishes for $x_3 > R$, as well as $\tilde{Y}^s(.,y)$, and then $U^s_{Y,1}(\cdot,y) - U^s_{Y,2}(\cdot,y)$ vanishes for $x_3 > R$. Unique continuation for elasticity implies that $U^s_{Y,1}(\cdot,y)$ and $U^s_{Y,2}(\cdot,y)$ coincide in the unbounded component of the complement $\mathcal{O}$ of $\overline{\mathcal{D}_1 \cup \mathcal{D}_2}$ in W, for all $y \in S_R$.
Now we use the reciprocity lemma 2.15. This implies that for all $x \in \mathcal{O}$, the solutions $X^s_{\sigma,1}(\cdot,x)$ and $X^s_{\sigma,2}(\cdot,x)$ associated to incident wave $G^\sigma_u(\cdot,x)$ coincide on S_R. By using the same arguments as before, we conclude that $U^s_{\sigma,1}(x,y)$ and $U^s_{\sigma,2}(x,y)$ coincide for all $(x,y) \in O \times O$.
Assuming now that $\mathcal{D}_1 \neq \mathcal{D}_2$, there exists $x^* \in \partial\mathcal{D}_1$ with $x^* \notin \overline{\mathcal{D}_2}$ and the boundary $\partial\mathcal{D}_1$ is smooth at point x^*. For sufficiently large integer n, the point $x_n = x^* + \boldsymbol{\nu}_1(x^*)/n$ (where $\boldsymbol{\nu}_1$ is the outward unit normal to $\mathcal{D}_1$) belongs to $\mathcal{O}$.
Due to well-posedness of the direct scattering problem (2.14) satisfied by $U^s_{\sigma,2}(.,y)$ in $W \setminus \overline{\mathcal{D}_2}$ when y is not on $\partial\mathcal{D}_2$, we have

$$\lim_{n\to+\infty} U^s_{\sigma,2}(x^*,x_n) = U^s_{\sigma,2}(x^*,x^*).$$

On the other hand boundary condition on $\partial\mathcal{D}_1$ implies that $U^s_{\sigma,1}(x^*,x_n) = -G^\sigma_u(x^*,x_n)$, and due to the singularity of G^σ_u (see lemma 2.12) we have

$$\lim_{n\to+\infty} |U^s_{\sigma,1}(x^*,x_n)| = +\infty.$$

Here we have used the fact that the field $U^s_{\sigma,1}(.,x_n)$ is continuous up to the boundary near x^* due to standard regularity results for $C^{1,1}$ domains. This is a contradiction because $U^s_{\sigma,1}(x^*,x_n) = U^s_{\sigma,2}(x^*,x_n)$ for sufficiently large n. ■

Remark 3.2 *The reader may wonder why the following more classical reciprocity relationship was not used to prove uniqueness: for all $x, y \in W \setminus \overline{\mathcal{D}}$ we have*

$$U^s_\sigma(x,y) = {}^T U^s_\sigma(y,x),$$

where $U^s_\sigma(.,y)$ denotes the solution of the scattering problem (2.14) with $f = -G^\sigma_u(.,y)|_{\partial\mathcal{D}}$ for $y \in W \setminus \overline{\mathcal{D}}$. Actually, we cannot prove that if $U^s_\sigma(.,y)$ vanishes on S_R then it vanishes for $x_3 > R$, while such result holds with $X^s_\sigma(.,y)$ and $Y^s_\sigma(.,y)$.

Since we have proved the identifiability of the obstacle from our data, we can now describe the Linear Sampling Method based on the same data.
By denoting $\mathbf{L}^2(\hat{S})$ as $\mathbf{L}^2(S_{-R}) \times \mathbf{L}^2(S_R)$ in case (i) and $\mathbf{L}^2(\hat{S}) = \mathbf{L}^2(S_R)$ in case (ii), we consider the near field operator $F : \mathbf{L}^2(\hat{S}) \to \mathbf{L}^2(\hat{S})$ such that for $\mathbf{h} \in \mathbf{L}^2(\hat{S})$ we have

$$(F\mathbf{h})(x) = \int_{\hat{S}} X^s_Y(x,y)\mathbf{h}(y)ds(y), \qquad x \in \hat{S}.$$

Like in [9], the justification of the Linear Sampling Method is based on a factorization of the operator F.
We define the operator $B : \mathbf{H}^{\frac{1}{2}}(\partial\mathcal{D}) \to \mathbf{L}^2(\hat{S})$ for $\boldsymbol{f} \in \mathbf{H}^{\frac{1}{2}}(\partial\mathcal{D})$ by $B\boldsymbol{f} = (\mathcal{R}|_X \mathcal{E}|_{XY} \mathbf{u})\,|_{\hat{S}}$ where $\mathbf{u}$ is the solution to the scattering problem (2.14) with data $\boldsymbol{f}$.
Then we define $\mathcal{H} : \mathbf{L}^2(\hat{S}) \to \mathbf{H}^{\frac{1}{2}}(\partial\mathcal{D})$ by

$$(\mathcal{H}\mathbf{h})(x) = \int_{\hat{S}} G_u^Y(x,y)\mathbf{h}(y)ds(y), \qquad x \in \partial\mathcal{D}.$$

Lastly we define $\mathcal{F} : \mathbf{H}^{-\frac{1}{2}}(\partial\mathcal{D}) \to \mathbf{L}^2(\hat{S})$ by

$$(\mathcal{F}\boldsymbol{\phi})(x) = \int_{\partial\mathcal{D}} G_X^\sigma(x,y)\boldsymbol{\phi}(y)ds(y), \qquad x \in \hat{S},$$

and $S : \mathbf{H}^{-\frac{1}{2}}(\partial\mathcal{D}) \to \mathbf{H}^{\frac{1}{2}}(\partial\mathcal{D})$ by

$$(S\boldsymbol{\phi})(x) = \int_{\partial\mathcal{D}} G_u^\sigma(x,y)\boldsymbol{\phi}(y)ds(y), \qquad x \in \partial\mathcal{D}.$$

Introducing the assumption

Assumption (H): ω is not an eigenfrequency for the Lamé's system in $\mathcal{D}$,

we have the following

Lemma 3.3 *The operator S is an isomorphism if the assumption (H) is satisfied.*

Proof. We introduce the boundary integral operator

$$\begin{array}{rccc} S_0 : & \mathbf{H}^{-\frac{1}{2}}(\partial\mathcal{D}) & \to & \mathbf{H}^{\frac{1}{2}}(\partial\mathcal{D}) \\ & \phi & \mapsto & \displaystyle\int_{\partial\mathcal{D}} E(x,y)\boldsymbol{\phi}(y)ds(y). \end{array}$$

The operator S_0 is an isomorphism if the assumption (H) is satisfied, by comparison with the corresponding static case considered in [22]. The kernel of the operator $S - S_0$ is $G_u^\sigma(x,y) - E(x,y)$ and is smooth in W. The operator $S - S_0$ is then continuous from $\mathbf{H}^{-\frac{1}{2}}(\partial\mathcal{D})$ to $\mathbf{H}^{\frac{1}{2}}(\partial\mathcal{D})$, so is the operator S.
The proof of injectivity and surjectivity follows the lines of the proof in the acoustic case [8]. ■

With assumption (H) we readily obtain the factorizations

$$F = -B\mathcal{H}, \quad \mathcal{F} = BS,$$

which leads to

$$F = -\mathcal{F}S^{-1}\mathcal{H}.$$

For what follows we need the following lemma, the proof of which is simply obtained by analyzing the form of G given by proposition 2.11 in the two different cases $x_3 < y_3$ and $x_3 > y_3$.

Lemma 3.4 *Let us consider $x = (x_S, x_3)$, $y = (y_S, y_3)$ in W.*
For $x_3 > y_3$ we have

$$G_u^Y(\cdot, y) = -\sum_{n>0} \frac{1}{2} \mathbf{U}_n^+(x)^T \mathbf{X}_n^-(y).$$

For $x_3 < y_3$ we have

$$G_u^Y(\cdot, y) = -\sum_{n>0} \frac{1}{2} \mathbf{U}_n^-(x)^T \mathbf{X}_n^+(y).$$

Now we need the following properties of operators $\mathcal{H}$, $\mathcal{F}$ and F.

Proposition 3.5 *Suppose assumption (H) is true. The operators $\mathcal{H}$, $\mathcal{F}$ and F are compact, injective with dense range. We have also $\overline{\mathcal{H}^*} = -\mathcal{F}$.*

Proof. We give a proof in the full-aperture case (i). We would handle the other case similarly. Since its kernel is smooth on $\partial\mathcal{D} \times \hat{S}$, the operator $\mathcal{H}$ is compact.
Let us prove that the operator $\mathcal{H}$ is injective. Let $\mathbf{h} = (\mathbf{h}^-, \mathbf{h}^+) \in \mathbf{L}^2(\hat{S})$ such that $\mathbf{h}^- = -\sum_{n>0} a_n^- \boldsymbol{\mathcal{Y}}_n$ and $\mathbf{h}^+ = \sum_{n>0} a_n^+ \boldsymbol{\mathcal{Y}}_n$. Assume the function

$$\mathbf{v}_h(x) = \int_{\hat{S}} G_u^Y(x, y) \mathbf{h}(y) ds(y)$$

vanishes on $\partial\mathcal{D}$. Since it solves the Lamé's system in $\mathcal{D}$, the function $\mathbf{v}_h$ vanishes in $\mathcal{D}$ by using assumption (H) and then in W by unique continuation.
For $x = (x_S, x_3)$ such that $-R < x_3 < R$, by using lemma 3.4 it follows that

$$\begin{aligned}
\mathbf{v}_h(x) = &\int_{S_{-R}} \left(-\sum_{n>0} \frac{1}{2} \mathbf{U}_n^+(x)^T \mathbf{X}_n^-(y) \right) \left(-\sum_{n>0} a_n^- \boldsymbol{\mathcal{Y}}_n(y) \right) ds(y) \\
&+ \int_{S_R} \left(-\sum_{n>0} \frac{1}{2} \mathbf{U}_n^-(x)^T \mathbf{X}_n^+(y) \right) \left(\sum_{n>0} a_n^+ \boldsymbol{\mathcal{Y}}_n(y) \right) ds(y) \\
&= -\sum_{n>0} \frac{1}{2} e^{i\beta_n R} \left(a_n^- \mathbf{U}_n^+(x) + a_n^+ \mathbf{U}_n^-(x) \right).
\end{aligned}$$

By applying now the operator $\mathcal{R}|_X \mathcal{E}|_{XY}$ to the above equation we obtain

$$\mathcal{R}|_X \mathcal{E}|_{XY} \mathbf{v}_h(x) = -\sum_{n>0} \frac{1}{2} e^{i\beta_n R} \left(a_n^- \mathbf{X}_n^+(x) + a_n^+ \mathbf{X}_n^-(x) \right).$$

The radiation condition and the fact that $\mathbf{v}_h$ vanishes on two sections on the right and on the left side of the obstacle implies that $a_n^- = a_n^+ = 0$ for all $n > 0$, which is the result.
Now we prove that for $\boldsymbol{\phi} \in \mathbf{H}^{-\frac{1}{2}}(\partial\mathcal{D})$ and $\mathbf{h} \in \mathbf{L}^2(\hat{S})$,

$$\langle \mathcal{H}\mathbf{h}, \boldsymbol{\phi} \rangle_{\mathbf{H}^{\frac{1}{2}}(\partial\mathcal{D}), \mathbf{H}^{-\frac{1}{2}}(\partial\mathcal{D})} = -\left(\mathbf{h}, \overline{\mathcal{F}\overline{\boldsymbol{\phi}}} \right)_{\mathbf{L}^2(\hat{S})} = -(\mathbf{h}, \overline{\mathcal{F}}\boldsymbol{\phi})_{\mathbf{L}^2(\hat{S})},$$

that is $-\overline{\mathcal{F}}$ is the adjoint operator of $\mathcal{H}$. We have

$$\langle \mathcal{H}\mathbf{h}, \boldsymbol{\phi} \rangle_{\mathbf{H}^{\frac{1}{2}}(\partial\mathcal{D}),\mathbf{H}^{-\frac{1}{2}}(\partial\mathcal{D})} = \left\langle \int_{\hat{S}} G_u^Y(.,y)\mathbf{h}(y)\, ds(y), \boldsymbol{\phi} \right\rangle,$$

$$= (\text{by Fubini's theorem}) \int_{\hat{S}} \mathbf{h}(y) \left\langle {}^T G_u^Y(.,y), \boldsymbol{\phi} \right\rangle ds(y)$$

$$= (\text{symmetry property}) \int_{\hat{S}} \mathbf{h}(y) \langle -G_X^\sigma(y,.), \boldsymbol{\phi} \rangle \, ds(y) = -\int_{\hat{S}} \mathbf{h}(y)(\mathcal{F}\overline{\boldsymbol{\phi}})(y)\, ds(y),$$

which is the result.
Now we prove that $\mathcal{H}$ has dense range, which is equivalent to prove that $\mathcal{F}$ is injective. Let $\boldsymbol{\phi} \in \mathbf{H}^{-\frac{1}{2}}(\partial\mathcal{D})$ such that $\mathcal{F}\boldsymbol{\phi} = 0$ on $\hat{S}$, in particular on S_R. We remark that for $x_3 > R$ and $y \in \partial\mathcal{D}$,

$$G_X^\sigma(x,y) = \frac{1}{2} \sum_{n>0} \mathbf{X}_n^+(x)^T \mathbf{U}_n^-(y),$$

then

$$(\mathcal{F}\boldsymbol{\phi})(x) = \int_{\partial\mathcal{D}} G_X^\sigma(x,y)\boldsymbol{\phi}(y) ds(y) = \frac{1}{2} \sum_{n>0} e^{i\beta_n x_3} \boldsymbol{\mathcal{X}}_n(x_S) \left(\int_{\partial\mathcal{D}} \mathbf{U}_n^-(y).\boldsymbol{\phi}(y)\, ds(y) \right).$$

That $\mathcal{F}\boldsymbol{\phi} = 0$ on S_R implies that $\int_{\partial\mathcal{D}} \mathbf{U}_n^-(y)\boldsymbol{\phi}(y)\, ds(y)$ vanishes for all n and then that the function $x \mapsto \int_{\partial\mathcal{D}} G_X^\sigma(x,y)\boldsymbol{\phi}(y) ds(y)$ vanishes for all $x_3 > R$. By applying the operator $\mathcal{R}^x|_u\mathcal{E}^x|_{XY}$, we obtain that for all $x_3 > R$

$$\int_{\partial\mathcal{D}} G_u^\sigma(x,y)\boldsymbol{\phi}(y) ds(y) = 0$$

and the function above vanishes in $W \setminus \overline{\mathcal{D}}$ as well with the help of unique continuation, and then also on $\partial\mathcal{D}$ in the sense of trace. We conclude that $\boldsymbol{\phi} = 0$ by using the injectivity of operator S. Hence $\mathcal{H}$ has dense range. That $\mathcal{F} = -\overline{\mathcal{H}^*}$ implies that $\mathcal{F}$ is compact, injective with dense range. It follows by using the relationship $F = -\mathcal{F}S^{-1}\mathcal{H}$ that F is compact, injective with dense range. ■

We are now in a position to introduce the near field equation, namely: find $\mathbf{h}(\cdot,z,p) \in \mathbf{L}^2(\hat{S})$ such that

$$F\mathbf{h} = G_X^Y(\cdot,z).p, \tag{3.1}$$

where z is a sampling point of W between sections S_{-R_0} and S_{R_0}, $p \in \mathbb{R}^d$ is a polarization vector, with $|p| = 1$. It should be remarked that the function $g_{z,p} : x \mapsto G_X^Y(x,z).p$ is in $\mathbf{L}^2(\hat{S})$. Due to obvious dimensional consideration, the introduction of such polarization vector in necessary in the framework of elasticity while it was not in the framework of acoustics.
The LSM consists in finding a quasi-solution of equation (3.1) for each z and then in plotting the norm of $\mathbf{h}(\cdot,z,p)$, which happens to explode when z goes outside the obstacle $\mathcal{D}$. The LSM is partially justified by the following theorem.

Theorem 3.6 *We assume that assumption (H) is satisfied for an obstacle $\mathcal{D}$ with Lipschitz continuous boundary. Let F be the near field operator with kernel $X_Y^s(.,y)$ solution to the scattering problem (2.14) with $f = -G_u^Y(.,y)|_{\mathcal{D}}$.*
(1) If $z \in \mathcal{D}$, then for all $\varepsilon > 0$ there exists a solution $\mathbf{h}_\varepsilon \in \mathbf{L}^2(\hat{S})$ of the inequality

$$||F\mathbf{h}_\varepsilon(\cdot,z,p) - G_X^Y(\cdot,z).p||_{\mathbf{L}^2(\hat{S})} \leq \varepsilon$$

such that the function $\mathcal{H}\mathbf{h}_\varepsilon$ converges in $\mathbf{H}^{\frac{1}{2}}(\partial\mathcal{D})$ as $\varepsilon \to 0$.
Furthermore, for a given fixed ε, the function $\mathbf{h}_\varepsilon(.,z,p)$ satisfies

$$\lim_{z\to\partial\mathcal{D}} ||\mathbf{h}_\varepsilon(.,z,p)||_{\mathbf{L}^2(\hat{S})} = +\infty \text{ and } \lim_{z\to\partial\mathcal{D}} ||\mathcal{H}\mathbf{h}_\varepsilon(.,z,p)||_{\mathbf{H}^{\frac{1}{2}}(\partial\mathcal{D})} = +\infty.$$

(2) If $z \in W \setminus \overline{\mathcal{D}}$ then every solution $\mathbf{h}_\varepsilon(.,z,p) \in \mathbf{L}^2(\hat{S})$ of the inequality

$$||F\mathbf{h}_\varepsilon(.,z,p) - G_X^Y(.,z).p||_{\mathbf{L}^2(\hat{S})} \leq \varepsilon$$

satisfies

$$\lim_{\varepsilon\to 0} ||\mathbf{h}_\varepsilon(.,z,p)||_{\mathbf{L}^2(\hat{S})} = +\infty \text{ and } \lim_{\varepsilon\to 0} ||\mathcal{H}\mathbf{h}_\varepsilon(.,z,p)||_{\mathbf{H}^{\frac{1}{2}}(\partial\mathcal{D})} = +\infty.$$

The proof of the previous theorem is based on a factorization of the operator F and proposition 3.5. Since it is very similar to the proof in the acoustic case (see [7]), it is omitted.

3.2 The modal formulation

The aim of this section is to transform the classical near field equation (3.1) into a modal formulation as it was done in [8] in the acoustic case. More precisely, such formulation will be based on the solutions $\mathbf{U}_n^{s^\pm}$ to the scattering problem (2.14) with $\boldsymbol{f} = -\mathbf{U}_n^\pm|_{\partial\mathcal{D}}$ for $n > 0$, that is the incident waves are the guided modes.
For we take advantage of the particular form of the green function given by proposition 2.11. Let us consider the incident wave $U^i(.,y) = G_u^Y(.,y)$. By using lemma 3.4, we have for $x \in W_R$ and $y \in S_{-R}$

$$U^i(x,y) = -\sum_{n>0} \frac{1}{2} \mathbf{U}_n^+(x)^T \mathbf{X}_n^-(y),$$

while for $x \in W_R$ and $y \in S_R$

$$U^i(x,y) = -\sum_{n>0} \frac{1}{2} \mathbf{U}_n^-(x)^T \mathbf{X}_n^+(y).$$

The modal formulation relies on the following proposition.

Proposition 3.7 *For all $x \in W_R \setminus \overline{\mathcal{D}}$*
(i) if $y \in S_{-R}$ then

$$U_Y^s(x,y) = -\sum_{n>0} \frac{1}{2} \mathbf{U}_n^{s^+}(x)^T \mathbf{X}_n^-(y), \tag{3.2}$$

(i) if $y \in S_R$ then

$$U_Y^s(x,y) = -\sum_{n>0} \frac{1}{2} \mathbf{U}_n^{s^-}(x)^T \mathbf{X}_n^+(y). \tag{3.3}$$

Proof. The right-hand sides of (3.2) and (3.3) clearly solve the first, second and fourth equations of the scattering problem (2.14). Since by definition of $\mathbf{U}_n^{s^+}$ and $\mathbf{U}_n^{s^-}$, we have $\mathbf{U}_n^{s^+}(x) + \mathbf{U}_n^+(x) = 0$ and $\mathbf{U}_n^{s^-}(x) + \mathbf{U}_n^-(x) = 0$ on $\partial\mathcal{D}$, then the boundary condition $U_Y^s(.,y) + U^i(.,y) = 0$ on $\partial\mathcal{D}$ is also satisfied, which completes the proof. ■

Next, we project the equation of the LSM on the guided modes. We first analyze the full-aperture situation (case (i)), then the back-scattering situation (case (ii)). In the full-aperture situation, $\mathbf{h} = (\mathbf{h}^-, \mathbf{h}^+) \in \mathbf{L}^2(S_{-R}) \times \mathbf{L}^2(S_R)$ with the modal decomposition

$$\mathbf{h}^- = \sum_{n>0} h_n^- \boldsymbol{\mathcal{Y}}_n \qquad \text{and} \qquad \mathbf{h}^+ = -\sum_{n>0} h_n^+ \boldsymbol{\mathcal{Y}}_n.$$

From (3.2) and (3.3), we obtain for $y \in S_{-R}$

$$X_Y^s(x,y) = -\sum_{n>0} \frac{1}{2} \mathbf{X}_n^{s^+}(x)^T \mathbf{X}_n^-(y) = \frac{1}{2} \sum_{n>0} e^{i\beta_n R} \mathbf{X}_n^{s^+}(x)^T \boldsymbol{\mathcal{X}}_n(y_S),$$

and for $y \in S_R$

$$X_Y^s(x,y) = -\sum_{n>0} \frac{1}{2} \mathbf{X}_n^{s^-}(x)^T \mathbf{X}_n^+(y) = -\frac{1}{2} \sum_{n>0} e^{i\beta_n R} \mathbf{X}_n^{s^-}(x)^T \boldsymbol{\mathcal{X}}_n(y_S).$$

We have for $x \in \hat{S}$:

$$\begin{aligned} F\mathbf{h}(x) &= \int_{S_{-R}} X_Y^s(x,y) \mathbf{h}^-(y) ds(y) + \int_{S_R} X_Y^s(x,y) \mathbf{h}^+(y) ds(y) \\ &= \sum_{n>0} \frac{e^{i\beta_n R}}{2} \left(h_n^- \mathbf{X}_n^{s^+}(x) + h_n^+ \mathbf{X}_n^{s^-}(x) \right). \end{aligned}$$

For $x \in S_{-R}$ we can write

$$\mathbf{X}_n^{s^+} = \sum_{m>0} (A_n^+)_m^- \boldsymbol{\mathcal{X}}_m \text{ and } \mathbf{X}_n^{s^-} = \sum_{m>0} (A_n^-)_m^- \boldsymbol{\mathcal{X}}_m.$$

We obtain

$$F\mathbf{h}(x) = \sum_{m>0} \sum_{n>0} \frac{e^{i\beta_n R}}{2} \left((A_n^+)_m^- h_n^- + (A_n^-)_m^- h_n^+ \right) \boldsymbol{\mathcal{X}}_m(x_S).$$

For $x \in S_R$ we can write

$$\mathbf{X}_n^{s^+} = \sum_{m>0} (A_n^+)_m^+ \boldsymbol{\mathcal{X}}_m \text{ and } \mathbf{X}_n^{s^-} = \sum_{m>0} (A_n^-)_m^+ \boldsymbol{\mathcal{X}}_m.$$

We obtain

$$F\mathbf{h}(x) = \sum_{m>0} \sum_{n>0} \frac{e^{i\beta_n R}}{2} \left((A_n^+)_m^+ h_n^- + (A_n^-)_m^+ h_n^+ \right) \boldsymbol{\mathcal{X}}_m(x_S).$$

Considering now the right-hand side of the near field equation (3.1), we have for $x \in \hat{S}$ and for $z = (z_S, z_3) \in W$ such that $-R < -R_0 < z_3 < R_0 < R$,

$$G_X^Y(x,z).p = \sum_{m>0} \frac{e^{i\beta_m |x_3 - z_3|}}{2} \boldsymbol{\mathcal{X}}_m(x_S) \left(\boldsymbol{\mathcal{X}}_m(z_S).p \right).$$

Collecting all the results we obtain for all $m > 0$,

$$\begin{cases} \displaystyle\sum_{n>0} e^{i\beta_n R} \left((A_n^+)_m^- h_n^- + (A_n^-)_m^- h_n^+ \right) = e^{i\beta_m (R+z_3)} (\boldsymbol{\mathcal{X}}_m(z_S).p) \\ \displaystyle\sum_{n>0} e^{i\beta_n R} \left((A_n^+)_m^+ h_n^- + (A_n^-)_m^+ h_n^+ \right) = e^{i\beta_m (R-z_3)} (\boldsymbol{\mathcal{X}}_m(z_S).p), \end{cases} \tag{3.4}$$

which is the modal formulation we expected in the full-aperture situation.

In the back-scattering situation, let $\mathbf{h} \in \mathbf{L}^2(S_R)$ have the modal decomposition $\mathbf{h} = \sum_{n>0} h_n^+ \boldsymbol{\mathcal{Y}}_n$. The equation of the linear sampling method is: for all $m > 0$

$$\sum_{n>0} e^{i\beta_n R} (A_n^-)_m^+ h_n^+ = e^{i\beta_m (R-z_3)} (\boldsymbol{\mathcal{X}}_m(z_S).p). \tag{3.5}$$

It is important to note that we have up to now exploited the near field equation (3.1) obtained with a left-hand side based on G_X^Y, which is one of the four blocks of the extended Green tensor G given by proposition 2.11. It is clear that we similarly obtain three other near field equations if we use the other blocks G_Y^Y, G_Y^X and G_X^X of tensor G. It is not difficult to see that actually the blocks G_X^Y and G_Y^Y lead to the same near field equation, as well as the blocks G_Y^X and G_X^X, which means that only two different near field equations can be exploited.
Let us exhibit the second one, obtained for example with block G_Y^X. It is written for $\mathbf{h} \in \mathbf{L}^2(\hat{S})$ and $x \in \hat{S}$,

$$\int_{\hat{S}} Y_X^s(x,y) \mathbf{h}(y) ds(y) = G_Y^X(x,z).p,$$

where $Y_X^s(.,y) := \mathcal{R}^x|_Y \mathcal{E}^x|_{XY} U_X^s(.,y)$, and $U_X^s(.,y)$ is the scattered field due to the incident wave $G_u^X(.,y)$ for $y \in \hat{S}$.
In the full-aperture situation, we assume that $\mathbf{h} = (\mathbf{h}^-, \mathbf{h}^+) \in \mathbf{L}^2(S_{-R}) \times \mathbf{L}^2(S_R)$ has the modal decomposition

$$\mathbf{h}^- = \sum_{n>0} h_n^- \boldsymbol{\mathcal{X}}_n \qquad \text{and} \qquad \mathbf{h}^+ = \sum_{n>0} h_n^+ \boldsymbol{\mathcal{X}}_n,$$

while the scattered fields due to the guided modes have the following decomposition: for $x \in S_{-R}$

$$\mathbf{Y}_n^{s^+} = \sum_{m>0} (A_n^+)_m^- \boldsymbol{\mathcal{Y}}_m \text{ and } \mathbf{Y}_n^{s^-} = \sum_{m>0} (A_n^-)_m^- \boldsymbol{\mathcal{Y}}_m,$$

for $x \in S_R$

$$\mathbf{Y}_n^{s^+} = \sum_{m>0} (A_n^+)_m^+ \boldsymbol{\mathcal{Y}}_m \text{ and } \mathbf{Y}_n^{s^-} = \sum_{m>0} (A_n^-)_m^+ \boldsymbol{\mathcal{Y}}_m.$$

By reproducing the same calculations as above the near field equation becomes in the full-aperture situation: for all $m > 0$,

$$\begin{cases} \displaystyle\sum_{n>0} e^{i\beta_n R} \left((A_n^+)_m^- h_n^- + (A_n^-)_m^- h_n^+ \right) = e^{i\beta_m (R+z_3)} (\boldsymbol{\mathcal{Y}}_m(z_S).p) \\ \displaystyle\sum_{n>0} e^{i\beta_n R} \left((A_n^+)_m^+ h_n^- + (A_n^-)_m^+ h_n^+ \right) = e^{i\beta_m (R-z_3)} (\boldsymbol{\mathcal{Y}}_m(z_S).p), \end{cases} \tag{3.6}$$

while the near field equation in the back-scattering situation is: for all $m > 0$,

$$\sum_{n>0} e^{i\beta_n R} (A_n^-)_m^+ h_n^+ = e^{i\beta_m (R-z_3)} (\boldsymbol{\mathcal{Y}}_m(z_S).p). \tag{3.7}$$

As a conclusion, and whatever the situation concerning data (full-aperture or back-scattering), we obtain six different systems for $d = 3$, because we can solve two different near field equations (either (3.4) or (3.6) in the full-aperture situation), with three different polarization vectors, namely $p = (1, 0, 0)$, $p = (0, 1, 0)$ and $p = (0, 0, 1)$. For $d = 2$, which is the framework of our numerical experiments in the next section, we have only two different polarization vectors, namely $p = (1, 0)$ and $p = (0, 1)$, which leads to four different systems. By specifying the left-hand side in each case for $d = 2$, we obtain four different polarizations: system (3.4) with $p = (1, 0)$ will be referred to as polarization t_1, system (3.4) with $p = (0, 1)$ as polarization u_3, system (3.6) with $p = (1, 0)$ as polarization u_1, and system (3.6) with $p = (0, 1)$ as polarization t_3.

4 Numerical experiments

Our numerical experiments are conducted in the two dimensional setting, namely $d = 2$, with section $S = (-0.5, 0.5)$. The material we consider is steel, the Lamé's constants λ and μ are deduced from the associated Young's modulus $E = 210$ GPa and Poisson's ratio $\nu = 0.3$, while the density is $\rho = 7932\,\mathrm{kg.m}^{-3}$. The obstacle we consider is formed by two spheres: the first one is centered at $(-0.2, 0.2)$ and has radius 0.05, the second one is centered at $(0.3, 0)$ and has radius 0.07. Note that such obstacle is the same as chosen in the acoustic case [8], so that a comparison between the results obtained in acoustics and those obtained in elasticity is possible. We set $R_0 = 1$, that is we try to retrieve the obstacle within the sampling grid $(-1, 1) \times (-0.5, 0.5)$, which is the domain of the sampling point z in the Linear Sampling Method.
We obtain some artificial data, that is $(\mathbf{X}_n^{s^\pm}, \mathbf{Y}_n^{s^\pm})$ on $\hat{S}$, by using a finite element method based on a weak formulation of problem (2.14). Such method is detailed in [6]. More

specifically, we use $P2$ classical Lagrange elements based on a triangulation such that the mesh size is consistent with the smallest wavelength involved in the problem. Some artificial noisy data are produced by applying to the scattering data $(\mathbf{X}_n^{s^\pm}, \mathbf{Y}_n^{s^\pm})$ obtained with our forward computations some Gaussian noise of various amplitude. More precisely, exactly as in [8], we compute at each point of the discretized fields $(\mathbf{X}_n^{s^\pm}, \mathbf{Y}_n^{s^\pm})$ some Gaussian noise with normal distribution. This pointwise perturbation is multiplied by a constant which is calibrated in order to obtain a relative L^2 error of prescribed amplitude, that is 1%, 5%, 10%, 20%.

For obvious reasons, solving each system (3.4), (3.5), (3.6) and (3.7) requires to restrict m and n to finite numbers. As already mentioned before, the guided modes are divided into propagative modes and non-propagative (inhomogeneous or evanescent) modes. It was extensively shown in [8] for the acoustic case that taking the non-propagative modes into account in the LSM increased the instability of the inverse problem, which led us to stick to the propagative modes in the modal formulation. We do the same choice in the present study: m and n will range from 1 to N_p, where N_p is the number of propagative modes at a given frequency ω. With such restriction to a finite number of modes, solving the systems (3.4), (3.5), (3.6) and (3.7) amounts to inverting some square matrices of dimension N_p in the back-scattering situation and of dimension $2N_p$ in the full-aperture situation. Since such inversions are unstable due to the ill-posedness of the problem in the continuous setting (because operator F is compact), we apply the Tikhonov/Morozov regularization as introduced in [14]. More precisely, we apply exactly the same method as detailed in [8] for the acoustic case. In all the figures that follow, we represent the level curves of function $\log(1/||\mathbf{h}(z)||_{\mathbf{L}^2(\hat{S})})$, where $\mathbf{h}(z)$ is the Tikhonov/Morozov's regularized solution, when z describes the sampling grid, so that the retrieved obstacle is the set of points z for which such function does not vanish.

In the remainder of the paper, we analyze the impact of some various parameters on the efficiency of the imaging method, essentially the number of incident waves, the amplitude of noise and the direction of polarization. We also test the method in the case of cracks, since such a case is important in the context of non destructive evaluation.

4.1 Influence of the number of incident waves

The dispersive relationship given in appendix A provides for each frequency ω the Lamb modes $(\beta_n, \boldsymbol{\mathcal{X}}_n, \boldsymbol{\mathcal{Y}}_n)$ for $n > 0$, and in particular the number N_p of propagative modes. The number N_p is given as a function of ω in the table below

ω	60	74	100	124	140	188
N_p	10	12	16	20	22	30

.

The figures 2 and 3 represent, in the full-aperture case and the back-scattering case respectively, the identification results obtained with polarization u_3 for 1% noise and increasing number N_p. As expected, the quality of the reconstruction increases with the number of propagative modes that are injected in the method. In particular, it is better in the full-aperture case than in the back-scattering case.

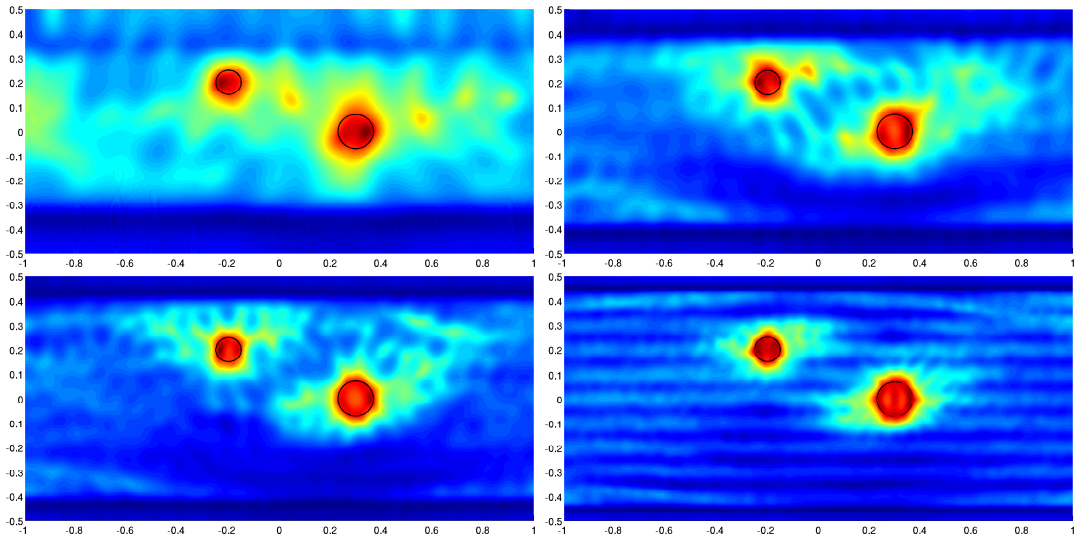

Figure 2: Full-aperture, 1% noise, $N_p = 10$ (top left), $N_p = 16$ (top right), $N_p = 20$ (bottom left), $N_p = 30$ (bottom right)

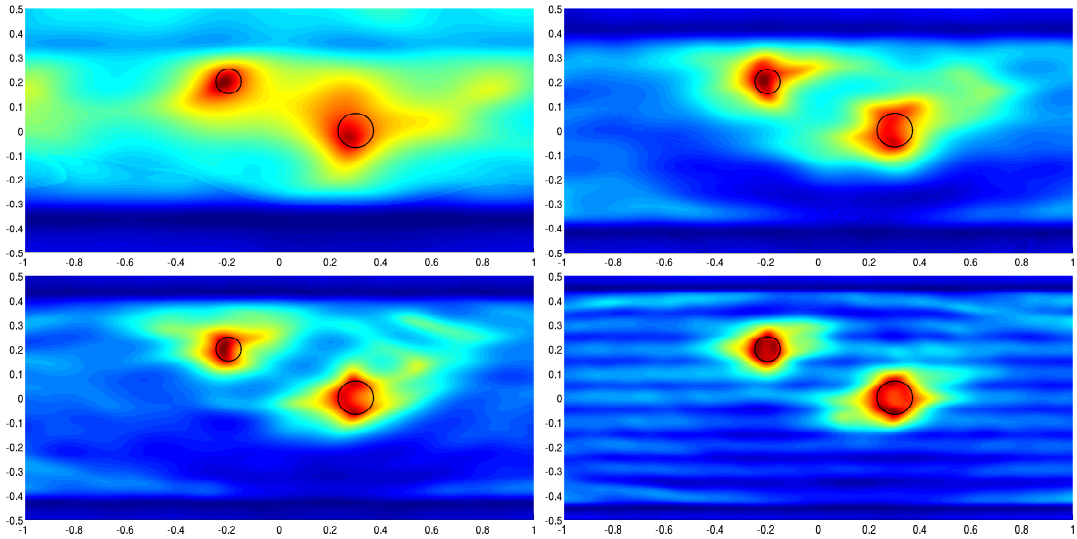

Figure 3: Back-scattering, 1% noise, $N_p = 10$ (top left), $N_p = 16$ (top right), $N_p = 20$ (bottom left), $N_p = 30$ (bottom right)

4.2 Influence of the amplitude of noise

In this study $N_p = 20$ is chosen, note that in such case the smallest wavelength associated to the guided modes is of the same order than the size of the spheres. The figures 4 and 5 represent, in the full-aperture case and the back-scattering case respectively, the identification results obtained with polarization u_3 for increasing amplitude of noise. We

conclude that the identification results are quite robust with respect to Gaussian noise.

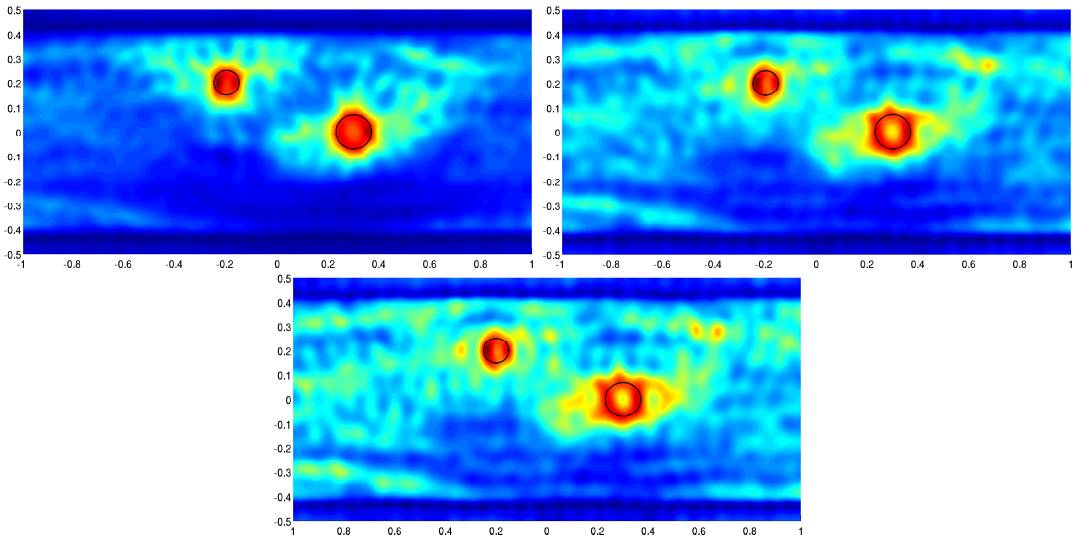

Figure 4: Full-aperture, $N_p = 20$, increasing noise: 1% noise (top left), 10% noise (top right), 20% noise (bottom)

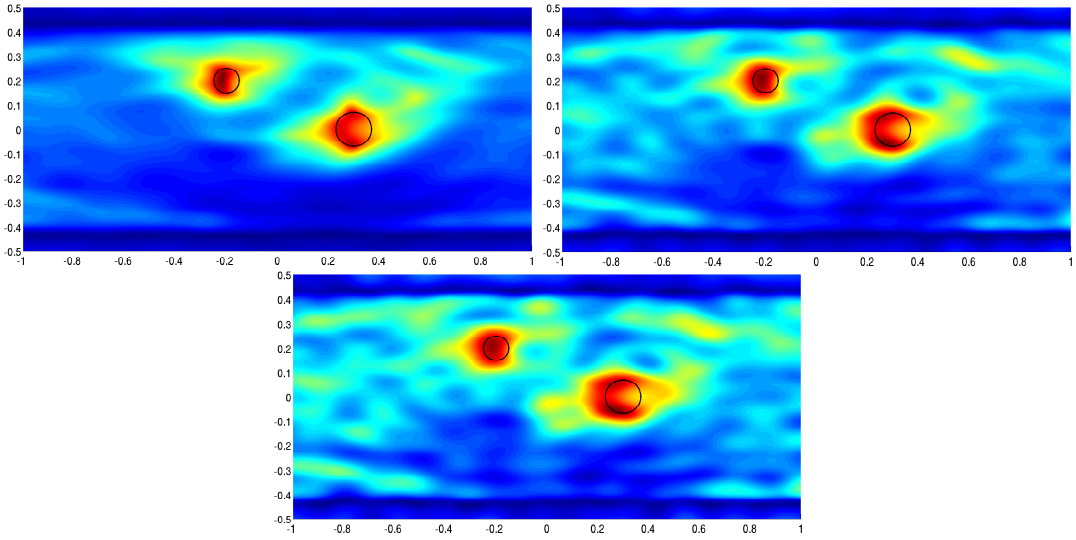

Figure 5: Back-scattering, $N_p = 20$, increasing noise: 1% noise (top left), 10% noise (top right), 20% noise (bottom)

4.3 Influence of the polarization

At the end of subsection 3.2, we identified four different polarizations depending on the near field equation we choose (either 3.4 ou 3.6 in the full-aperture case) and on the

polarization vector in the left-hand side of such equation ($p = (1, 0)$ or $p = (0, 1)$). On figure 6, we have displayed the identification results obtained in the full-aperture case, for $N_p = 20$ and 1% noise, with our four different polarizations. We remark that each polarization provides approximately the same quality of reconstruction.

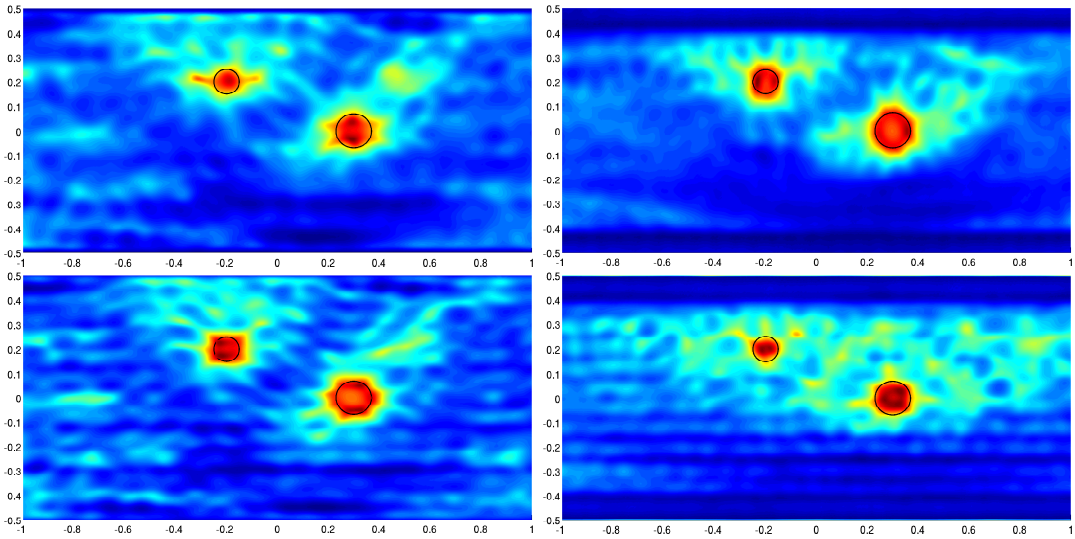

Figure 6: Full-aperture, 1% noise, $N_p = 20$, different polarizations: t_1 (top left), u_3 (top right), u_1 (bottom left) t_3 (bottom right)

4.4 Identification of cracks

We complete this numerical section with a test of our method when the defect is no more an obstacle characterized by vanishing displacement $\mathbf{u} = 0$, but is now a linear crack characterized by vanishing traction $\sigma(\mathbf{u})\boldsymbol{\nu} = 0$. Obviously the case of cracks is important in the field of ultrasonic NDT. This kind of defect does not fit the theoretical framework of the present paper, which concerns only the case of hard obstacles. We hence provide here some numerical results without theoretical analysis, which is however probably feasible also in the case of cracks by adapting the arguments given in [10] to the elastic waveguide.

We see on the following figures 7 and 8 the identification results for a linear crack from point $(0, 0)$ to point $(0.15, 0.15)$ in the full-aperture and the back-scattering cases, with $N_p = 12$ and polarization u_3, for two different amplitudes of noise. We see on figures 9 and 10 the same results but for a linear crack from point $(0, 0.5)$ to point $(0.15, 0.35)$. Note that this second crack meets the upper boundary of the waveguide, which is a shortcoming as far as accessibility is concerned but which frequently occurs in applications. As expected the results are less satisfactory for this second crack than for the first one.

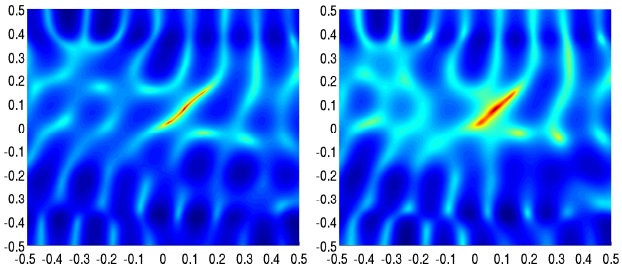

Figure 7: Full-aperture, $N_p = 12$, 1% noise (left) and 5% noise (right)

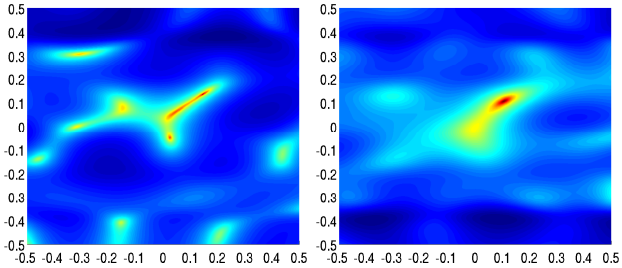

Figure 8: Back-scattering, $N_p = 12$, 1% noise (left), 5% noise (right)

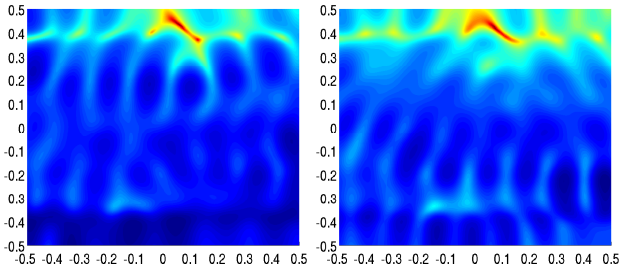

Figure 9: Full-aperture, $N_p = 12$, 1% noise (left), 5% noise (right)

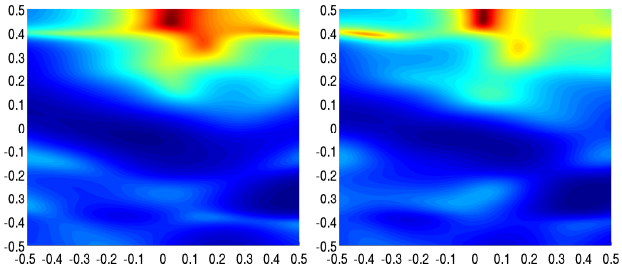

Figure 10: Back-scattering, $N_p = 12$, 1% noise (left), 5% noise (right)

Appendix A : the Lamb modes in 2D

Note that the 3D case reduces to the 2D case if we consider the thick plate $W = \{x \in \mathbb{R}^3,\ -h < x_1 < h\}$ with invariance following variable x_2, and if we restrict to the $P - SV$

modes, that is we do not consider the SH modes (see [5]). In the 2D case the Lamb modes β_n satisfy the dispersive relationship (see [26]):

$$t^2\cos(\alpha_P h+\kappa)\sin(\alpha_S h+\kappa)+4\beta^2\alpha_P\alpha_S\cos(\alpha_S h+\kappa)\sin(\alpha_P h+\kappa)=0,$$

where we have

$$c_S=\sqrt{\frac{\mu}{\rho}},\quad c_P=\sqrt{\frac{\lambda+2\mu}{\rho}},$$
$$k_S=\frac{\omega}{c_S},\quad k_P=\frac{\omega}{c_P},$$
$$\alpha_S=\sqrt{k_S^2-\beta^2},\quad \alpha_P=\sqrt{k_P^2-\beta^2},\quad t=\alpha_S^2-\beta^2.$$

Here, $\kappa=0$ corresponds to symmetric modes while $\kappa=\dfrac{\pi}{2}$ corresponds to the antisymmetric modes. The associated displacement is:

$$\begin{cases} u_1(x_1)=\dfrac{\alpha_P}{t}\dfrac{\sin(\alpha_P x_1+\kappa)}{\cos(\alpha_P h+\kappa)}-\dfrac{1}{2\alpha_S}\dfrac{\sin(\alpha_S x_1+\kappa)}{\cos(\alpha_S h+\kappa)} \\ u_3(x_1)=\dfrac{-i\beta}{t}\dfrac{\cos(\alpha_P x_1+\kappa)}{\cos(\alpha_P h+\kappa)}+\dfrac{1}{2i\beta}\dfrac{\cos(\alpha_S x_1+\kappa)}{\cos(\alpha_S h+\kappa)}. \end{cases}$$

The components $(\boldsymbol{t}_S,-t_3)$ are given by Hooke's law $\sigma(\boldsymbol{u}_S,u_3)e_3=(\boldsymbol{t}_S,-t_3)$, that is

$$\begin{cases} t_1(x_1)=\mu(i\beta u_1+\dfrac{\partial u_3}{\partial x_1}) \\ t_3(x_1)=-(\lambda+2\mu)i\beta u_3-\lambda\dfrac{\partial u_1}{\partial x_1}. \end{cases}$$

Lastly, the Fraser's constant is given by

$$J=\int_{-h}^{h}(t_1u_1+t_3u_3)\,dx_1.$$

Appendix B : proof of proposition 2.11

The proof relies on a construction of G column by column. By using assumption (2.6) we have the expansion

$$\begin{cases} G_X^X(\cdot,y)e_1=\sum_{n>0}a_n^1(x_3)\boldsymbol{\mathcal{X}}_n(x_S) \\ G_Y^X(\cdot,y)e_1=\sum_{n>0}b_n^1(x_3)\boldsymbol{\mathcal{Y}}_n(x_S). \end{cases}$$

Plugging such modal expansion of $G_X^X(\cdot,y)e_1$ and $G_Y^X(\cdot,y)e_1$ in equation (2.16) we obtain:

$$\begin{cases} \sum_{n>0}\left(\dfrac{da_n^1}{dx_3}(x_3)-i\beta_n b_n^1(x_3)\right)\boldsymbol{\mathcal{X}}_n(x_S)=\begin{pmatrix}1\\0\\0\end{pmatrix}\delta(x_3-y_3)\delta(x_S-y_S), \\ \sum_{n>0}\left(\dfrac{db_n^1}{dx_3}(x_3)-i\beta_n a_n^1(x_3)\right)\boldsymbol{\mathcal{Y}}_n(x_S)=0. \end{cases}$$

We multiply the first equation by $\boldsymbol{\mathcal{Y}}_n(x_S)$ and the second equation by $\boldsymbol{\mathcal{X}}_n(x_S)$, we integrate over S and we get with the help of biorthogonality, for all $n > 0$:

$$\left\{ \begin{array}{l} \dfrac{da_n^1}{dx_3}(x_3) - i\beta_n b_n^1(x_3) = u_1^n(y_S)\delta(x_3 - y_3), \\ \dfrac{db_n^1}{dx_3}(x_3) - i\beta_n a_n^1(x_3) = 0. \end{array} \right.$$

We hence derive the equation

$$\frac{d^2 b_n^1}{dx_3^2}(x_3) + \beta_n^2 b_n^1(x_3) = i\beta_n u_1^n(y_S)\delta(x_3 - y_3). \tag{4.1}$$

We hence conclude that for all $n > 0$

$$\left\{ \begin{array}{ll} b_n^1(x_3) = A_n^- e^{-i\beta_n(x_3-y_3)} + B_n^- e^{i\beta_n(x_3-y_3)} & x_3 < y_3 \\ b_n^1(x_3) = A_n^+ e^{-i\beta_n(x_3-y_3)} + B_n^+ e^{i\beta_n(x_3-y_3)} & x_3 > y_3 \end{array} \right.$$

and

$$\left\{ \begin{array}{ll} a_n^1(x_3) = -A_n^- e^{-i\beta_n(x_3-y_3)} + B_n^- e^{i\beta_n(x_3-y_3)} & x_3 < y_3 \\ a_n^1(x_3) = -A_n^+ e^{-i\beta_n(x_3-y_3)} + B_n^+ e^{i\beta_n(x_3-y_3)} & x_3 > y_3. \end{array} \right.$$

The radiation condition implies that

$$\left\{ \begin{array}{ll} T^+ G_Y^X = G_X^X & x_3 = R \\ T^- G_Y^X = -G_X^X & x_3 = -R \end{array} \right.$$

that is

$$\left\{ \begin{array}{ll} b_n^1(x_3) = a_n^1(x_3) & x_3 > y_3 \\ b_n^1(x_3) = -a_n^1(x_3) & x_3 < y_3 \end{array} \right.$$

and lastly $A_n^+ = 0 = B_n^-$. The remaining constants $A_n := A_n^-$ and $B_n := B_n^+$ are obtained by using equation (4.1). We finally obtain

$$\left\{ \begin{array}{l} a_n^1(x_3) = s(x_3 - y_3)\dfrac{u_1^n(y_S)}{2} e^{i\beta_n|x_3-y_3|} \\ b_n^1(x_3) = \dfrac{u_1^n(y_S)}{2} e^{i\beta_n|x_3-y_3|}. \end{array} \right.$$

The same technique is used to obtain the other five columns of G, namely

$$\left(\begin{array}{c} G_X^X(\cdot,y)e_2 \\ G_Y^X(\cdot,y)e_2 \end{array} \right), \left(\begin{array}{c} G_X^X(\cdot,y)e_3 \\ G_Y^X(\cdot,y)e_3 \end{array} \right), \left(\begin{array}{c} G_X^Y(\cdot,y)e_1 \\ G_Y^Y(\cdot,y)e_1 \end{array} \right), \left(\begin{array}{c} G_X^Y(\cdot,y)e_2 \\ G_Y^Y(\cdot,y)e_2 \end{array} \right), \left(\begin{array}{c} G_X^Y(\cdot,y)e_3 \\ G_Y^Y(\cdot,y)e_3 \end{array} \right).$$

Appendix C : proof of lemma 2.14

The proof is very similar to the one given in the acoustic case (see [8], appendix B). We reproduce it in the elastic case because of the specific treatment of the radiation condition. We define for $x \in \Omega := W \setminus \overline{\mathcal{D}}$ some $r > 0$ such that $B(x, 2r) \subset \Omega$. By

following the lines of the proof in the acoustic case, we first obtain by using lemma 2.13 that

$$\mathbf{u}(x) + \int_{\partial B(x,r)} (\gamma_\nu^y(G_u^\sigma(x,y))\mathbf{u}(y) - G_u^\sigma(x,y)\gamma_\nu \mathbf{u}(y))\, ds(y) = 0, \tag{4.2}$$

where $\boldsymbol{\nu}$ is oriented inside $B(x,r)$. Now we use the Green formula in the subdomain Ω_R of $\Omega \setminus \overline{B(x,r)}$ lying between sections S_{-R} and S_R. We have

$$\begin{aligned}
0 = \int_{\Omega_R} \left((\mathrm{div}(\sigma(G_u^\sigma(x,y)) + \rho\omega^2 G_u^\sigma(x,y))\mathbf{u}(y) - G_u^\sigma(x,y)(\mathrm{div}(\sigma(\mathbf{u}) + \rho\omega^2\mathbf{u})(y)\right) dy \\
= \int_{\partial\mathcal{D}} (\gamma_\nu^y(G_u^\sigma(x,y))\mathbf{u}(y) - G_u^\sigma(x,y)\gamma_\nu\mathbf{u}(y))\ ds(y) \\
+ \int_{\partial B(x,r)} (\gamma_\nu^y(G_u^\sigma(x,y))\mathbf{u}(y) - G_u^\sigma(x,y)\gamma_\nu\mathbf{u}(y))\ ds(y) \\
+ \int_{\Gamma_R} (\gamma_\nu^y(G_u^\sigma(x,y))\mathbf{u}(y) - G_u^\sigma(x,y)\gamma_\nu\mathbf{u}(y))\ ds(y) \\
+ \int_{S_{-R}} (\gamma_\nu^y(G_u^\sigma(x,y))\mathbf{u}(y) - G_u^\sigma(x,y)\gamma_\nu\mathbf{u}(y))\ ds(y) \\
+ \int_{S_R} (\gamma_\nu^y(G_u^\sigma(x,y))\mathbf{u}(y) - G_u^\sigma(x,y)\gamma_\nu\mathbf{u}(y))\ ds(y).
\end{aligned}$$

The integral on Γ_R vanishes because of the boundary condition on ∂W. Consider now the last integral on S_R. We denote $\mathbf{X} = (\mathbf{t}_S, \mathsf{u}_3)$, $\mathbf{Y} = (\mathbf{u}_S, \mathsf{t}_3)$ and $\mathbf{X}_j^g = (\mathbf{t}_{S,j}^g, \mathsf{u}_{3,j}^g)$, $\mathbf{Y}_j^g = (\mathbf{u}_{S,j}^g, \mathsf{t}_{3,j}^g)$ the mixed variables associated to $\mathbf{u}$ and $G_{u,j}^\sigma$ respectively, where $G_{u,j}^\sigma$ is the $j-th$ line of tensor G_u^σ. We have

$$\begin{aligned}
\int_{S_R} \left(\gamma_\nu^y(G_{u,j}^\sigma(x,y)).\mathbf{u}(y) - G_{u,j}^\sigma(x,y).\gamma_\nu\mathbf{u}(y)\right)\ ds(y) \\
= \int_{S_R} \Big((\mathbf{t}_{S,j}^g.\mathbf{u}_S - \mathsf{t}_{3,j}^g\mathsf{u}_3) - (\mathbf{t}_S.\mathbf{u}_{S,j}^g - \mathsf{t}_3\mathsf{u}_{3,j}^g)\Big)\ ds(y) \\
= \int_{S_R} \Big((\mathbf{t}_{S,j}^g.\mathbf{u}_S + \mathsf{u}_{3,j}^g\mathsf{t}_3) - (\mathbf{t}_S.\mathbf{u}_{S,j}^g + \mathsf{u}_3\mathsf{t}_{3,j}^g)\Big)\ ds(y) = (\mathbf{X}_j^g|\mathbf{Y})_{S_R} - (\mathbf{X}|\mathbf{Y}_j^g)_{S_R}.
\end{aligned}$$

Now we use the radiation condition $\mathbf{X}_j^g = T^+\mathbf{Y}_j^g$ and $\mathbf{X} = T^+\mathbf{Y}$. By definition of T^+, we have

$$(\mathbf{X}_j^g|\mathbf{Y})_{S_R} = (T^+\mathbf{Y}_j^g|\mathbf{Y})_{S_R} = \sum_{n>0} (\boldsymbol{\mathcal{X}}_n|\mathbf{Y}_j^g)_{S_R}(\boldsymbol{\mathcal{X}}_n|\mathbf{Y})_{S_R} = (\mathbf{X}|\mathbf{Y}_j^g)_{S_R}$$

and the integral on S_R vanishes for all j. For the same reason, the integral on S_{-R} vanishes as well for all j.
We hence have

$$\begin{aligned}
\int_{\partial\mathcal{D}} (\gamma_\nu^y(G_u^\sigma(x,y))\mathbf{u}(y) - G_u^\sigma(x,y)\gamma_\nu\mathbf{u}(y))\ ds(y) = \\
- \int_{\partial B(x,r)} (\gamma_\nu^y(G_u^\sigma(x,y))\mathbf{u}(y) - G_u^\sigma(x,y)\gamma_\nu\mathbf{u}(y))\ ds(y),
\end{aligned}$$

which together with equation (4.2) completes the proof.

Appendix D : proof of lemma 2.15

By lemma 2.14 and using $G_u^\sigma(x,y) = {}^T G_u^\sigma(y,x)$ we have

$$U_Y^s(x,y) = \int_{\partial\mathcal{D}} (\gamma_\nu^z(G_u^\sigma(x,z))U_Y^s(z,y) - G_u^\sigma(x,z)\gamma_\nu^z(U_Y^s(z,y)))\, ds(z)$$

$$= \int_{\partial\mathcal{D}} \Big(\gamma_\nu^z({}^T G_u^\sigma(z,x))U_Y^s(z,y) - {}^T G_u^\sigma(z,x)\gamma_\nu^z(U_Y^s(z,y))\Big)\, ds(z). \tag{4.3}$$

We have also

$$U_\sigma^s(y,x) = \int_{\partial\mathcal{D}} (\gamma_\nu^z(G_u^\sigma(y,z))U_\sigma^s(z,x) - G_u^\sigma(y,z)\gamma_\nu^z(U_\sigma^s(z,x)))\, ds(z).$$

By applying operator $\mathcal{R}^x|_X\mathcal{E}^x|_{XY}$, we obtain

$$X_\sigma^s(y,x) = \int_{\partial\mathcal{D}} (\gamma_\nu^z(G_X^\sigma(y,z))U_\sigma^s(z,x) - G_X^\sigma(y,z)\gamma_\nu^z(U_\sigma^s(z,x)))\, ds(z),$$

and by applying transposition

$${}^T X_\sigma^s(y,x) = -\int_{\partial\mathcal{D}} \Big(\gamma_\nu^z({}^T U_\sigma^s(z,x)){}^T G_X^\sigma(y,z) - {}^T U_\sigma^s(z,x)\gamma_\nu^z({}^T G_X^\sigma(y,z))\Big)\, ds(z).$$

Now the relationship $G_u^Y(x,y) = -{}^T G_X^\sigma(y,x)$ implies

$${}^T X_\sigma^s(y,x) = \int_{\partial\mathcal{D}} \Big(\gamma_\nu^z({}^T U_\sigma^s(z,x))G_u^Y(z,y) - {}^T U_\sigma^s(z,x)\gamma_\nu^z(G_u^Y(z,y))\Big)\, ds(z).$$

If we use the Green formula of lemma 2.13 outside $\mathcal{D}$ for two displacement fields formed by the $i-th$ column of $U_\sigma^s(.,x)$ and the $j-th$ column of $U_Y^s(.,y)$, for $i,j = 1...d$, we obtain

$$\int_{\partial\mathcal{D}} \Big(\gamma_\nu^z({}^T U_\sigma^s(z,x))U_Y^s(z,y) - {}^T U_\sigma^s(z,x)\gamma_\nu^z(U_Y^s(z,y))\Big)\, ds(z) = 0,$$

which by summation with the previous equation and setting $\tilde{G}_u^Y(x,y) = G_u^Y(x,y) + U_Y^s(x,y)$ implies

$${}^T X_\sigma^s(y,x) = \int_{\partial\mathcal{D}} \Big(\gamma_\nu^z({}^T U_\sigma^s(z,x))\tilde{G}_u^Y(z,y) - {}^T U_\sigma^s(z,x)\gamma_\nu^z(\tilde{G}_u^Y(z,y))\Big)\, ds(z).$$

We also have

$$\int_{\partial\mathcal{D}} \Big(\gamma_\nu^z({}^T G_u^\sigma(z,x))G_u^Y(z,y) - {}^T G_u^\sigma(z,x)\gamma_\nu^z(G_u^Y(z,y))\Big)\, ds(z) = 0,$$

which by summation with (4.3) implies

$$U_Y^s(x,y) = \int_{\partial\mathcal{D}} \Big(\gamma_\nu^z({}^T G_u^\sigma(z,x))\tilde{G}_u^Y(z,y) - {}^T G_u^\sigma(z,x)\gamma_\nu^z(\tilde{G}_u^Y(z,y))\Big)\, ds(z).$$

We conclude by defining $\tilde{G}_u^\sigma(x,y) = G_u^\sigma(x,y) + U_\sigma^s(x,y)$ that

$$U_Y^s(x,y) + {}^T X_\sigma^s(y,x) = \int_{\partial\mathcal{D}} \Big(\gamma_\nu^z({}^T \tilde{G}_u^\sigma(z,x))\tilde{G}_u^Y(z,y) - {}^T \tilde{G}_u^\sigma(z,x)\gamma_\nu^z(\tilde{G}_u^Y(z,y))\Big)\, ds(z).$$

It follows that $U_Y^s(x,y) + {}^T X_\sigma^s(y,x) = 0$ since $\tilde{G_u^Y}(\cdot,y)$ and ${}^T\tilde{G}_u^\sigma(\cdot,x)$ vanish on $\partial\mathcal{D}$.

References

[1] C. J. S. Alves and R. Kress, *On the far-field operator in elastic obstacle scattering*, IMA J. Appl. Math., 67 (2002), pp. 1–21.

[2] T. Arens, *Why linear sampling works*, Inverse Problems, 20 (2004), pp. 163–173.

[3] T. Arens and A. Lechleiter, *The linear sampling method revisited*, J. Integral Equations Appl., 21 (2009), pp. 179–202.

[4] K. Baganas, B. B. Guzina, A. Charalambopoulos, and G. D. Manolis, *A linear sampling method for the inverse transmission problem in near-field elastodynamics*, Inverse Problems, 22 (2006), pp. 1835–1853.

[5] V. Baronian, *Couplage des méthodes modale et éléments finis pour la diffraction des ondes élastiques guidées*, Thèse, Ecole Polytechnique, Paris, 2009.

[6] V. Baronian, A.-S. Bonnet-BenDhia, and E. Lunéville, *Transparent boundary conditions for the harmonic diffraction problem in an elastic waveguide*, J. Comput. Appl. Math, (2009), pp. 1945–1952.

[7] L. Bourgeois and E. Lunéville, *The linear sampling method in a waveguide: a formulation based on modes*, Journal of Physics: Conference Series, 135 (2008), p. 012023.

[8] ——, *The linear sampling method in a waveguide: a modal formulation*, Inverse Problems, 24 (2008), p. 015018.

[9] F. Cakoni and D. Colton, *On the mathematical basis of the linear sampling method*, Georgian Math. J., 10 (2003), pp. 411–425. Dedicated to the 100th birthday anniversary of Professor Victor Kupradze.

[10] ——, *Qualitative methods in inverse scattering theory*, Interaction of Mechanics and Mathematics, Springer-Verlag, Berlin, 2006. An introduction.

[11] A. Charalambopoulos, D. Gintides, and K. Kiriaki, *The linear sampling method for the transmission problem in three-dimensional linear elasticity*, Inverse Problems, 18 (2002), pp. 547–558.

[12] T. J. Christiansen and M. Taylor, *Inverse problems for obstacles in a waveguide*, Communications in Partial Differential Equations, 35 (2010), pp. 328–352.

[13] D. Colton and A. Kirsch, *A simple method for solving inverse scattering problems in the resonance region*, Inverse Problems, 12 (1996), pp. 383–393.

[14] D. Colton, M. Piana, and R. Potthast, *A simple method using morozov's discrepancy principle for solving inverse scattering problems*, Inverse Problems, 13 (1997), pp. 1477–1493.

[15] S. Dediu and J. R. Mc Laughlin, *Recovering inhomogeneities in a waveguide using eigensystem decomposition*, Inverse Problems, 22 (2006), pp. 1227–1246.

[16] G. Eskin, J. Ralston, and M. Yamamoto, *Inverse scattering for gratings and wave guides*, Inverse Problems, 24 (2008), p. 025008.

[17] W. B. Fraser, *Orthogonality relation for the rayleigh-lamb modes of vibration of a plate*, J. Acoust. Soc. Am., 59 (1976), pp. 215–216.

[18] D. Gintides and K. Kiriaki, *The far-field equations in linear elasticity—an inversion scheme*, ZAMM Z. Angew. Math. Mech., 81 (2001), pp. 305–316.

[19] B. B. Guzina and A. I. Madyarov, *A linear sampling approach to inverse elastic scattering in piecewise-homogeneous domains*, Inverse Problems, 23 (2007), pp. 1467–1493.

[20] C. Hazard and M. Lenoir, *Formulations variationnelles pour le diffraction des ondes électromagnétiques*, Rapport de recherche 339, Ecole Nationale Supérieure de Techniques Avancées, Paris, 2000.

[21] A. Kirsch and N. Grinberg, *The factorization method for inverse problems*, vol. 36 of Oxford Lecture Series in Mathematics and its Applications, Oxford University Press, Oxford, 2008.

[22] W. McLean, *Strongly elliptic systems and boundary integral equations*, Cambridge University Press, Cambridge, 2000.

[23] S. Nintcheu Fata and B. B. Guzina, *A linear sampling method for near-field inverse problems in elastodynamics*, Inverse Problems, 20 (2004), pp. 713–736.

[24] V. Pagneux and A. Maurel, *Lamb wave propagation in elastic waveguides with variable thickness*, Proc. R. Soc. Lond. Ser. A Math. Phys. Eng. Sci., 462 (2006), pp. 1315–1339.

[25] R. Potthast, *Point sources and multipoles in inverse scattering theory*, vol. 427 of Chapman & Hall/CRC Research Notes in Mathematics, Chapman & Hall/CRC, Boca Raton, FL, 2001.

[26] F. Royer Daniel and E. Dieulesaint, *Ondes élastiques dans les solides*, Interaction of Mechanics and Mathematics, Masson, Paris, 1996. Tomes 1, Propagation libre et guidée.